spectrum was invariant from −40 to +25 °C when measured in toluene-d_8.

Acknowledgment. For support of this research, we thank the Division of Basic Energy Sciences of the Department of Energy. We also thank the Camille and Henry Dreyfus Foundation for a Teacher-Scholar Grant and the Alfred P. Sloan Foundation for a Research Fellowship (to W.J.E.).

Registry No. 2a, 90762-81-5; **2a′**, 90742-67-9; **3a**, 80642-73-5; **4** (R = *t*-C_4H_9), 80642-66-6; **5**, 90742-68-0; $[(C_5H_5)_2YD(THF)]_2$, 80642-74-6; $[(C_5H_5)_2Y(CH_3)_2Li(THF)_2$, 90742-70-4; $[(CH_3C_5H_4)_2YH(THF)]_2$, 80658-44-2; $[(CH_3C_5H_4)_2ZrH_2]_2$, 77965-67-4; $(C_5H_5)_3Y(THF)$, 79533-63-4.

The Design of Multianionic Chelating Ligands for the Production of Inorganic Oxidizing Agents. Osmium Coordination Chemistry That Provides Stable Potent Oxidizing Agents and Stable Potent Reducing Agents

Fred C. Anson, Judith A. Christie, Terrence J. Collins,* Robert J. Coots, Tracy T. Furutani, Stephen L. Gipson, John T. Keech, Terry E. Krafft, Bernard D. Santarsiero,[1] and George H. Spies

Contribution No. 6881 from the The Chemical Laboratories, California Institute of Technology, Pasadena, California 91125. *Received December 9, 1983*

Abstract: The design of multianionic chelating ligands for use in producing new oxidizing agents is discussed. Two potentially tetradentate tetraanionic ligands, 1,2-bis(3,5-dichloro-2-hydroxybenzamido)ethane (H_4CHBA-Et (**1**)) and 1,2-bis(3,5-dichloro-2-hydroxybenzamido)-4,5-dichlorobenzene (H_4CHBA-DCB (**2**)) were synthesized and found to coordinate to osmium as tetradentate tetraanions. X-ray crystal structures of two osmium(IV) complexes of this ligand class are reported: octahedral Os(η^4-CHBA-Et)(py)$_2$ (**5**) has axial pyridine ligands with the tetradentate tetraanion coordinated to the equatorial positions, whereas in Os(η^4-CHBA-DCB)(bpy) (**15**) the bpy ligand occupies one axial and one equatorial position with one phenolic donor in an axial position and the remaining donors of the tetradentate tetraanion coordinated equatorially. Ligand **1** forms osmium complexes in oxidation states II, III, IV, and VI. Attempted electrooxidation of the osmium(IV) complex, **5**, to an osmium(V) complex results in oxidation of the tetradentate tetraanion at the ethylene unit bridging the amide nitrogen atoms. In the presence of alcohol or water this oxidation proceeds in a stepwise manner and several key intermediates have been isolated, independently synthesized, and characterized. The first intermediate isolated results from dehydrogenation of the ligand bridge. In the second intermediate, the unsaturated bridge has been oxidized to a 1,2 diether. Finally, cleavage of the carbon–carbon bond and dealkylation of the two ethereal oxygen atoms yields two bidentate ligands bound through phenolic and organic imido donors. The cleavage product is produced as two diastereomers which differ in the coordination geometry at the metal. Both isomers have been characterized by X-ray crystal structure determinations. The diastereomeric distribution is determined primarily by the nature of the alcohol employed. The ligand oxidation can be prevented by replacement of the ethylene unit of **1** with the dichlorophenylene moiety of **2**. Osmium complexes of **2** have been produced in oxidation states II, III, IV, VI, and presumably the very rare state V. The apparent osmium(V) complexes are stable but are potent oxidizing agents with potentials for the V/IV couples ranging from ca. 1.31 to 1.65 V vs. NHE. The complex [Os(η^4-CHBA-DCB)(*t*-Bupy)$_2$]$^+$ forms as an apparent mixture of two diastereomers. The stable osmium(II) complexes of both ligands **1** and **2** are potent reducing agents.

The variety of useful inorganic oxidizing agents presently available is limited by the lack of appropriate oxidation resistant ligands. We have initiated an attempt to prepare a series of strongly oxidizing complexes by designing and synthesizing new oxidation-resistant ligands. Most suitable known ligands are monodentate species in which the donor atom is electronegative (e.g., O^{2-}, Cl^-, F^-). Noteworthy exceptions include the η^2-peroxo and η^4-porphyrinato dianionic ligands.[2,3] Our approach has been to prepare multianionic chelating ligands that are capable of forming stable strongly oxidizing complexes and to investigate the coordination chemistry of the ligands and the reaction chemistry of their metal complexes. Many classical oxidizing agents (e.g., CrO_3, $KMnO_4$) exhibit poor chemoselectivity when oxidizing organic substrates. For some reactions a fundamental reason for this behavior is that additional metal-based oxidizing agents are formed during the redox process which oxidize the organic substrate in a manner different from the initial oxidizing agent. An example is the chromic acid oxidation of cyclobutanol in which chromium(VI) cleanly oxidizes cyclobutanol to cyclobutanone, but the chromium(IV) generated in this process also attacks the cyclobutanol and produces ring cleavage. The final inorganic product is chromium(III).[4] We believe that in searching for selective transition-metal oxidizing agents it is highly desirable to seek or design systems which allow one to *control oxidation state changes* at the metal site during an oxidation process. In particular, we wish to generate complexes that will undergo a single oxidation reaction with a specific organic substrate to give a

---

(1) Myron A. Bantrell Research Fellow, 1981–1983, the California Institute of Technology.

(2) For recent examples of the use of highly oxidized porphyrin complexes in oxidation reactions see: (a) Groves, J. T.; Watanabe, Y.; McMurry, T. J. *J. Am. Chem. Soc.* **1983**, *105*, 4489. (b) Groves, J. T.; Takahashi, T. *Ibid.* **1983**, *105*, 2073. (c) Smegal, J. A.; Schardt, B. C.; Hill, C. L. *Ibid.* **1983**, *105*, 3510. (d) Smegal, J. A.; Hill, C. L. *Ibid.* **1983**, *105*, 3515.

(3) The extremely oxidized complexes $[Fe(bpy)_3]^{4+}$ and $[Ru(bpy)_3]^{4+}$ have recently been produced electrochemically in liquid SO_2 showing that aromatic ligands are capable of forming observable complexes that are potent oxidizing agents. Gaudiello, J. G.; Sharp, P. R.; Bard, A. J. *J. Am. Chem. Soc.* **1982**, *104*, 6373. Stable very highly oxidizing complexes have recently been reported. Sharp, P. R.; Bard, A. J. *Inorg. Chem.* **1983**, *22*, 2689.

(4) Benson, D. "Mechanisms of Oxidation by Metal Ions"; Elsevier: New York, 1976, pp 178–193.

Scheme I

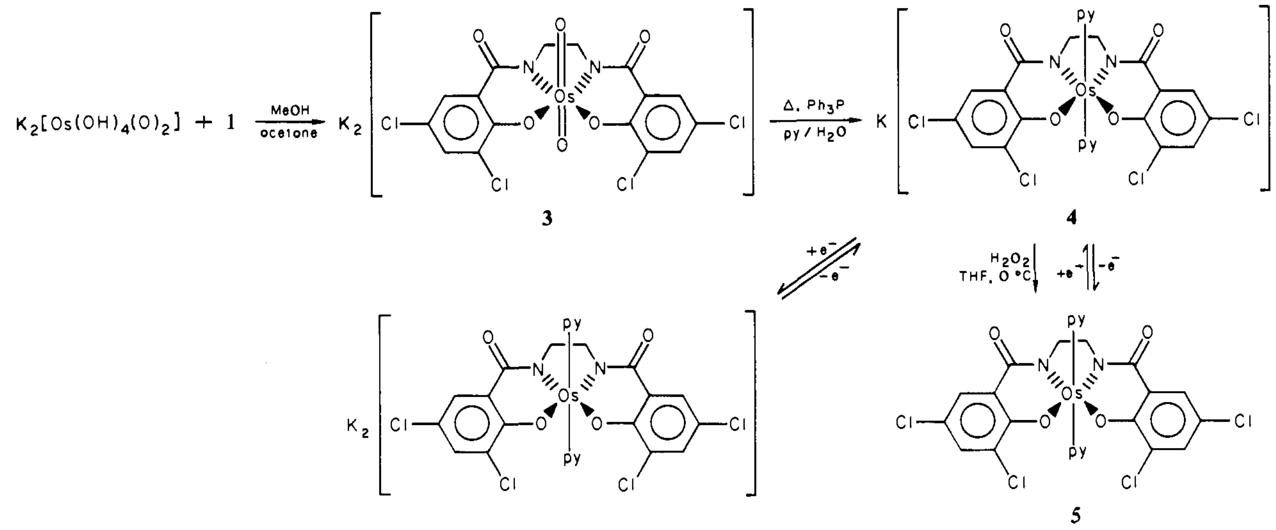

nonactive reduced inorganic product. Multianionic chelating ligands might provide the stabilization of the reduced inorganic product that is necessary for the achievement of this goal.

An important primary goal in our work has been to define the necessary structural features that make a multianionic chelating ligand compatible with very oxidizing metal centers and the environment necessary to generate them. These features include (i) resistance to oxidation, (ii) the formation of five- and six-membered metallacycles upon coordination, (iii) negative charge sufficient to counter the positive charge of the metal center, (iv) chemically innocent binding sites that are resistant to hydrolysis and other displacement reactions, (v) ease of derivatization to vary the oxidizing power of the complex and to incorporate steric bulk or chiral centers to achieve regio-, enantio-, and stereoselective transformations, and (vi) convenient syntheses that will facilitate the use of interesting complexes. The complexes may need to be coordinatively unsaturated to allow the substrate to coordinate prior to oxidation or to facilitate reactions which expand the coordination shell such as β-hydrogen transfer.

Two ligands that have been designed and examined as possible candidates are the potentially tetradentate, tetraanionic ligands H_4CHBA-Et (**1**) and H_4CHBA-DCB (**2**).[5,6] Note that these ligands contain organic amide functional groups which when N-coordinated are known to shift formal potentials of metal complexes to less positive values, i.e., to stabilize the higher oxidation state.[7-9] The chlorine substituents were introduced to protect the aromatic rings from oxidation.

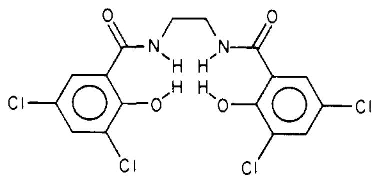

1

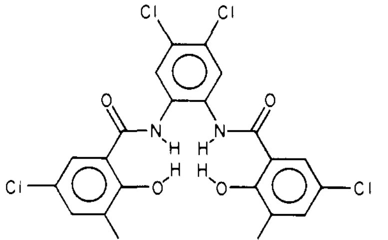

2

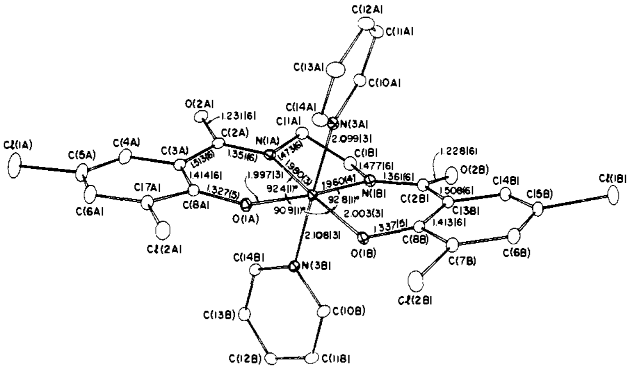

Figure 1. Molecular structure of Os(η^4-CHBA-Et)(py)$_2$ (**5**).

Here we report that it is possible to coordinate **1** and **2** as tetradentate tetraanions to osmium and that stable highly reducing complexes of **1** and **2** and highly oxidizing complexes of **2** can be produced. Osmium complexes in the oxidation states II, III, IV, V, and VI are described. It is shown that **1** and **2** meet the criteria listed above with the exception that **1** is not sufficiently resistant to oxidation to allow formation of a strongly oxidizing complex. The site of oxidative sensitivity in complexes of **1** has been identified as the ethylene unit bridging the two organic amide nitrogens. It is important to note that it is a simple matter to block this oxidation of the ligand by replacing the ethylene group with the more robust dichlorophenylene unit of **2**. Osmium is a particularly useful test metal since complexes in several of the higher oxidation states yield readily observable NMR spectra, a pleasant contrast with other metals we have investigated. This has proved

---

(5) Ligand names are 1,2-bis(3,5-dichloro-2-hydroxybenzamido)ethane, H_4CHBA-Et (**1**); 1,2-bis(3,5-dichloro-2-hydroxybenzamido)-4,5-dichlorobenzene, H_4CHBA-DCB (**2**); 1,2-bis(3,5-dichloro-2-hydroxybenzamido)ethylene, H_4CHBA-ethylene; 1,2-bis(3,5-dichloro-2-hydroxybenzamido)-*trans*-1,2-dimethoxyethane, H_4CHBA-*t*-1,2-diMeO-Et; *N*-formyl-3,5-dichloro-2-hydroxybenzamide, H_2Fo-CHBA. Abbreviations: py = pyridine; *t*-Bupy = 4-*tert*-butylpyridine; bpy = 2,2′-bipyridine; Ph_3P = triphenylphosphine; *t*-BuNC = *tert*-butyl isocyanide; TFA = trifluoroacetic acid; BPG = basal plane pyrolytic graphite; TBAP = tetrabutylammonium perchlorate; H_2OEP = octaethylporphyrin; SCE = saturated calomel electrode.

(6) (a) **1** forms a dimeric complex with chromium(III) in which both N-bound and O-bound organic amide ligands are found. Collins, T. J.; Santarsiero, B. D.; Spies, G. H. *J. Chem. Soc., Chem. Commun.* **1983**, 681. (b) Coordination of **1** as a tetradentate tetraanion to osmium(IV) has been reported. Christie, J. A.; Collins, T. J.; Krafft, T. E.; Santarsiero, B. D.; Spies, G. H. *J. Chem. Soc., Chem. Commun.* **1984**, 198.

(7) Sigel, H.; Martin, R. B. *Chem. Rev.* **1982**, *82*, 385.

(8) The use of multianionic chelating ligands containing organic amide functional groups to stabilize Cu(III) and Ni(III) has been extensively studied. (a) Margerum, D. W. *Pure Appl. Chem.* **1983**, *55*, 23. (b) Diaddario, L. L.; Robinson, W. R.; Margerum, D. W. *Inorg. Chem.* **1983**, *22*, 1021. (c) Kimura, E.; Sakonaka, A.; Machila, R.; Kodama, M. *J. Am. Chem. Soc.* **1982**, *104*, 4255.

(9) (a) Buttafava, A.; Fabbrizzi, L.; Perotti, A.; Seghi, B. *J. Chem. Soc., Chem. Commun.* **1982**, 1166. (b) Fabbrizzi, L.; Perotti, A.; Poggi, A. *Inorg. Chem.* **1983**, *22*, 1411.

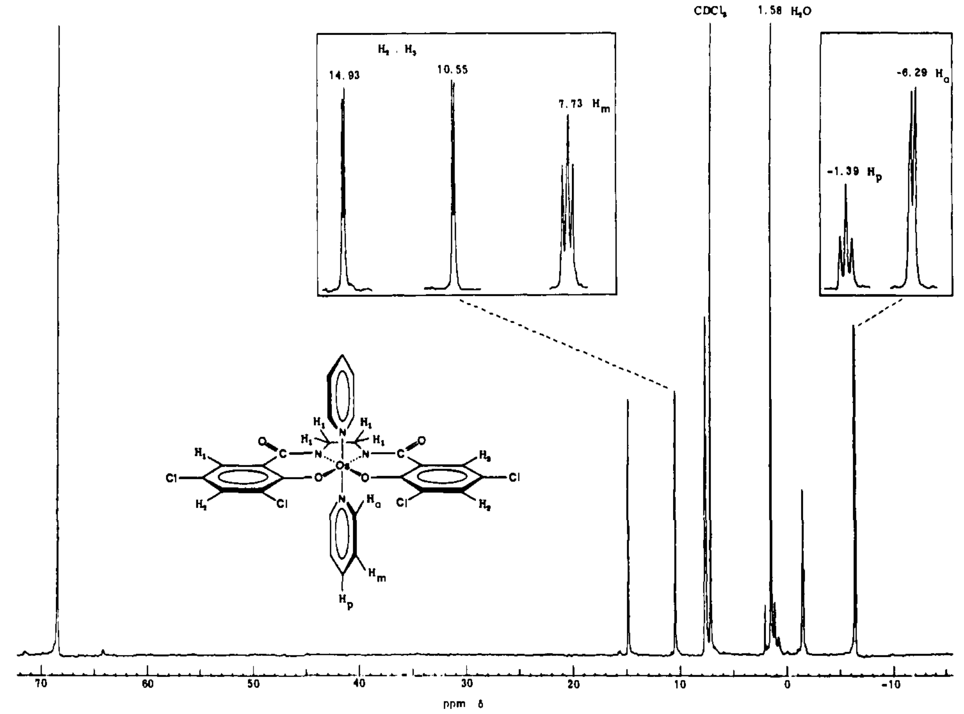

Figure 2. 90-MHz ^1H NMR spectrum of **5** ($CDCl_3$).

indispensible in characterizing the complexes described here.

Results and Discussion

Synthesis and Oxidation of an Os(IV) Complex of Ligand 1. The ligands **1** and **2** can be synthesized in high yields from readily available starting materials and familiar organic reactions. Osmium insertion into **1** can be achieved quantitatively as shown in Scheme I. The orange osmium(VI) complex $K_2[Os(\eta^4\text{-CHBA-Et})(O)_2]$ (**3**) contains trans-oxo ligands, as established by IR. Like other d^2 trans-dioxo osmium(VI) complexes this material is diamagnetic[10] and provides a reference for NMR spectroscopy. The IR and ^1H NMR data require equatorial coordination of the ligand **1** as a tetradentate tetraanion. Once bound in this fashion the ligand remains coordinated through a variety of chemical transformations. In all of the complexes described in this paper the ligand has thus far shown no sensitivity to hydrolysis or other displacement reactions. Complex **3** can be reduced by triphenylphosphine in the presence of pyridine to produce the paramagnetic osmium(III) complex $K[Os(\eta^4\text{-CHBA-Et})(py)_2]$ (**4**), and oxidation of **4** gives the deep blue neutral paramagnetic osmium(IV) complex $Os(\eta^4\text{-CHBA-Et})(py)_2$ (**5**) in high yield.

Complex **5** has been characterized by an X-ray crystal structure determination (Figure 1). This is the first structural study of an osmium(IV) pyridine complex. We recently reported on an Os(IV) dimer of ligand **1** which contained the first structurally characterized examples of Os(IV) bearing the N-coordinated organic amido ligand or the phenoxide ligand.[6b] In **5** the ligand **1** is coordinated as a tetradentate tetraanion to the equatorial positions of a distorted octahedron. The two pyridine ligands occupy the axial positions with a relative dihedral angle of 73°. It has been concluded that the relative orientation of *trans*-pyridine ligands in $Co(acac)_2(py)_2$ and $Ni(acac)_2(py)_2$, staggered for the former and eclipsed for the latter, is a function of crystal packing effects.[11] The paramagnetic complex **5** exhibits a well-resolved ^1H NMR spectrum as shown in Figure 2. Spectra of this type have been previously observed for osmium(IV) complexes.[12] The signal for the bridging ethylene protons is a singlet at 68.55 ppm.

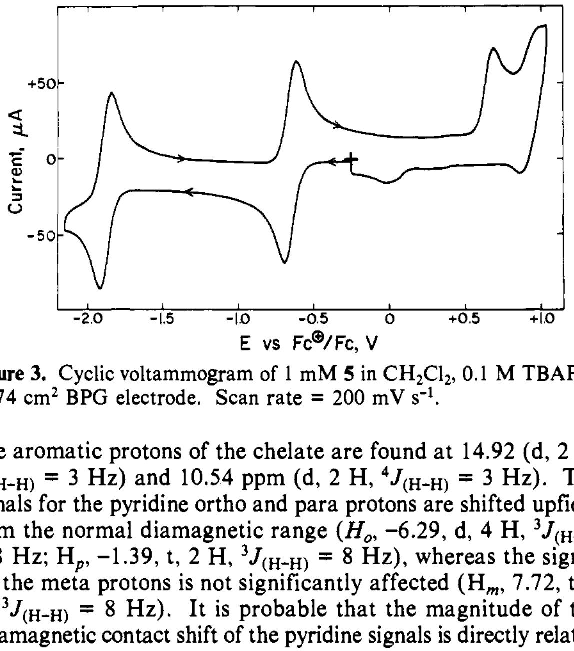

Figure 3. Cyclic voltammogram of 1 mM **5** in CH_2Cl_2, 0.1 M TBAP at 0.174 cm^2 BPG electrode. Scan rate = 200 mV s^{-1}.

The aromatic protons of the chelate are found at 14.92 (d, 2 H, $^4J_{(H-H)}$ = 3 Hz) and 10.54 ppm (d, 2 H, $^4J_{(H-H)}$ = 3 Hz). The signals for the pyridine ortho and para protons are shifted upfield from the normal diamagnetic range (H_o, −6.29, d, 4 H, $^3J_{(H-H)}$ = 8 Hz; H_p, −1.39, t, 2 H, $^3J_{(H-H)}$ = 8 Hz), whereas the signal for the meta protons is not significantly affected (H_m, 7.72, t, 4 H, $^3J_{(H-H)}$ = 8 Hz). It is probable that the magnitude of the paramagnetic contact shift of the pyridine signals is directly related to the nature of the second LUMO of pyridine, $3B_1$, which is composed of p orbitals on nitrogen and on the ortho and para positions, but not the meta positions.[13]

Cyclic voltammetry was used to probe the redox chemistry of the new complexes and the oxidative stability of the coordinated ligands. A typical cyclic voltammogram of **5** (1 mM in CH_2Cl_2, 0.1 M TBAP[5]) at a BPG[5] electrode is shown in Figure 3. Potentials were measured against the ferrocinium/ferrocene (Fc^+/Fc) couple which we have consistently measured as ca. 0.48 V vs. SCE[5] in the same medium. Two reversible diffusion-controlled one-electron responses having formal potentials of −0.65 and −1.88 V are found. In addition, two irreversible responses appear at E_p = +0.70 V and ca. 1.00 V. Plots of peak current vs. the square root of scan rate rate over the range 20–500 mV s^{-1} are linear for the two reversible couples and the first oxidation, indicating

---

(10) Schroeder, M. *Chem. Rev.* **1980**, *80*, 187.

(11) Elder, R. C. *Inorg. Chem.* **1968**, *7*, 1117; **1968**, *7*, 2316.

(12) (a) Pawson, D.; Griffith, W. P. *J. Chem. Soc., Dalton Trans.* **1975**, 417. (b) Chatt, J.; Leigh, G. J.; Mingos, D. M. P.; Paske, R. J. *J. Chem. Soc. A* **1968**, 2636. (c) Randall, E. W.; Shaw, D. *J. Chem. Soc. A* **1969**, 2867.

(13) Jorgensen, W. L.; Salem, L. "The Organic Chemist's Book of Orbitals"; Academic Press: New York, 1973; p 265.

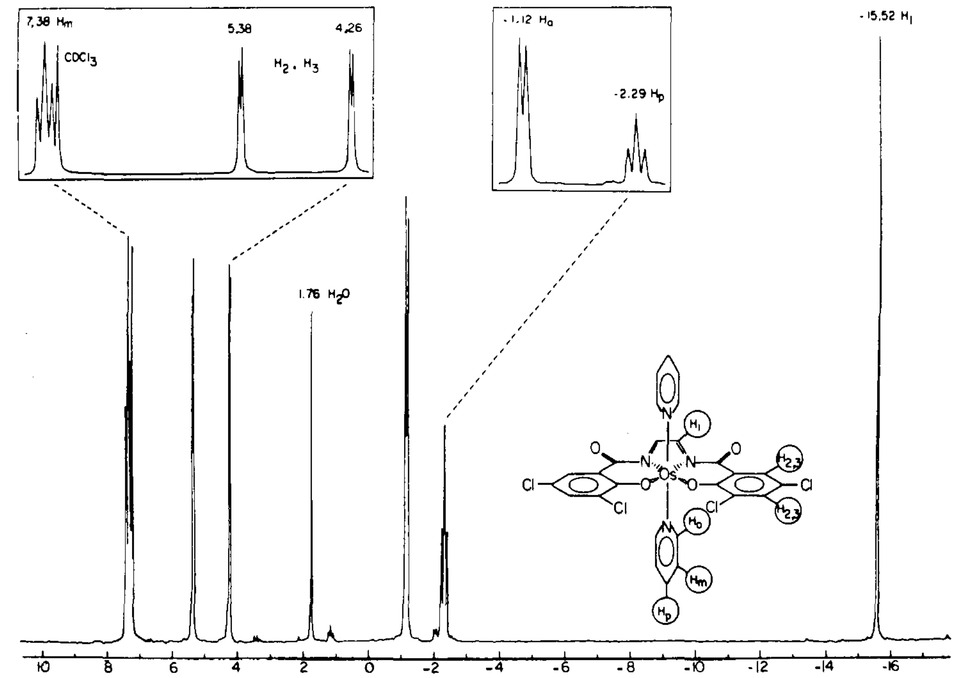

Figure 4. 90-MHz ^{1}H NMR spectrum of **7** ($CDCl_3$).

diffusion control. Controlled potential reduction of **5** at −0.90 V consumes one electron per molecule and produces **4** which can be reoxidized to pure **5**. Reduction of **5** in acetonitrile at −2.10 V consumes two electrons per molecule and produces a purple solution of the corresponding osmium(II) complex that is stable under an inert atmosphere. Exposure to air causes rapid formation of **4**. The formal potential of the osmium(III/II) couple, $[Os(\eta^4\text{-CHBA-Et})(py)_2]^{-/2-}$, −1.88 V, is almost 2 V more negative than that of the corresponding porphyrin complex, $[Os(\eta^4\text{-OEP})(py)_2]^{+/0}$, (0.0 V), in the same medium.[5,14] The osmium(II) complex $[Os(\eta^4\text{-CHBA-Et})(py)_2]^{2-}$ is thus a very powerful reducing agent. Clearly the tetraanionic ligand stabilizes osmium(III) much more strongly than does the dianionic octaethylporphyrinato ligand. We anticipate that this superior stabilization capacity will be a general property of the tetraanions.

The oxidative sensitivity of the ethylene unit bridging the amide nitrogens causes the oxidation of complex **5** to be irreversible. Electrochemical oxidation of **5** at 0.87 V in dichloromethane containing ROH (R = alkyl, H) (0.5 mol per mmol of osmium) consumes at least six electrons per osmium atom and gives quantitative conversion of **5** to either one of two new complexes, **9** and **9′**, or a mixture of both depending on the nature of R, vide infra (Scheme II). Thin-layer chromatography (TLC) of the anolyte solution monitored during the course of the electrolysis shows that the conversion proceeds through three distinct intermediates—**6**, **7**, and **8**. Comparison of TLC measurements when different alcohols are employed indicates that **6** and **8** contain the alcohol group while **7**, **9**, and **9′** do not. We wished to understand these transformations for two reasons. First, there is an obvious connection between the goals mentioned in the introduction and a knowledge of any oxidative reactions of a complex of the new ligand **1**. Second, it is possible to convert **9** and **9′** to active catalysts for electrooxidation of alcohols, and our studies of these catalytic systems required a knowledge of the structures of possible participant complexes.

It was inconvenient to separate and isolate the complex mixtures of osmium compounds that form during the electrolysis. Accordingly we sought separate chemical syntheses of the various intermediates and discovered that compound **7** can be quantitatively produced by autoxidation of **5** adsorbed on silica gel (Scheme II). The structure of **7** has been established by ^{1}H NMR (Table I and Figure 4) and ^{13}C NMR (Table II).[15] The signal for the methylene protons of the metallacyclopentane ring of **5** is found at 68.55 ppm, whereas the signal for the metallacyclopentene ring methine protons of **7** is found at −15.52 ppm. The five-membered

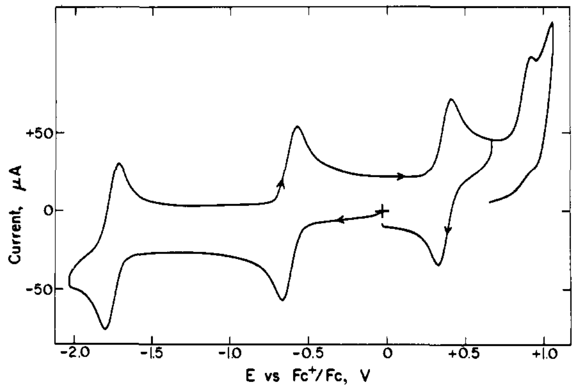

Figure 5. Cyclic voltammogram of 1 mM **7** in 0.1 M $TBAP/CH_2Cl_2$ at 0.174 cm^2 BPG electrode; scan rate = 200 mV s^{-1}.

unsaturated metallacycle of **7** can be represented by two contributing resonance structures in which the formal oxidation state of the metal is different. The cyclic voltammogram of **7** in the absence of alcohol is shown in Figure 5. Three reversible diffusion-controlled one-electron waves are found at E^f = −1.76, −0.62, and 0.37 V, and an irreversible oxidation is found at E_p = 0.92 V. The oxidation of **7** at 0.37 V is reversible in the absence of alcohols, but it becomes irreversible at low scan rates if alcohol is present. Electrochemical oxidation of **7** at 0.87 V in the presence of alcohol or water produces **8** and then **9** and/or **9′**. Complex

---

(14) Brown, G. M.; Hopf, F. R.; Meyer, T. J.; Whitten, D. G. *J. Am. Chem. Soc.* **1975**, *97*, 5385.

(15) A considerable number of ligand oxidative dehydrogenations have been previously reported. For examples of such reactions in osmium chemistry see: Lay, P. A.; Sargeson, A. M.; Skelton, B. W.; White, A. J. *J. Am. Chem. Soc.* **1982**, *104*, 6161 and references therein. Oxidation of methylene units attached to the nitrogen atoms of chelating N-coordinated polypeptides to copper(III) has been reported. Rybka, J. S.; Margerum, D. W. *Inorg. Chem.* **1981**, *20*, 1453 and references therein. For a recent review of α,α-diimine complexes including ligand oxidations see: Van Koten, G.; Vrieze, K. *Adv. Organomet. Chem.* **1982**, *21*, 151.

Scheme II

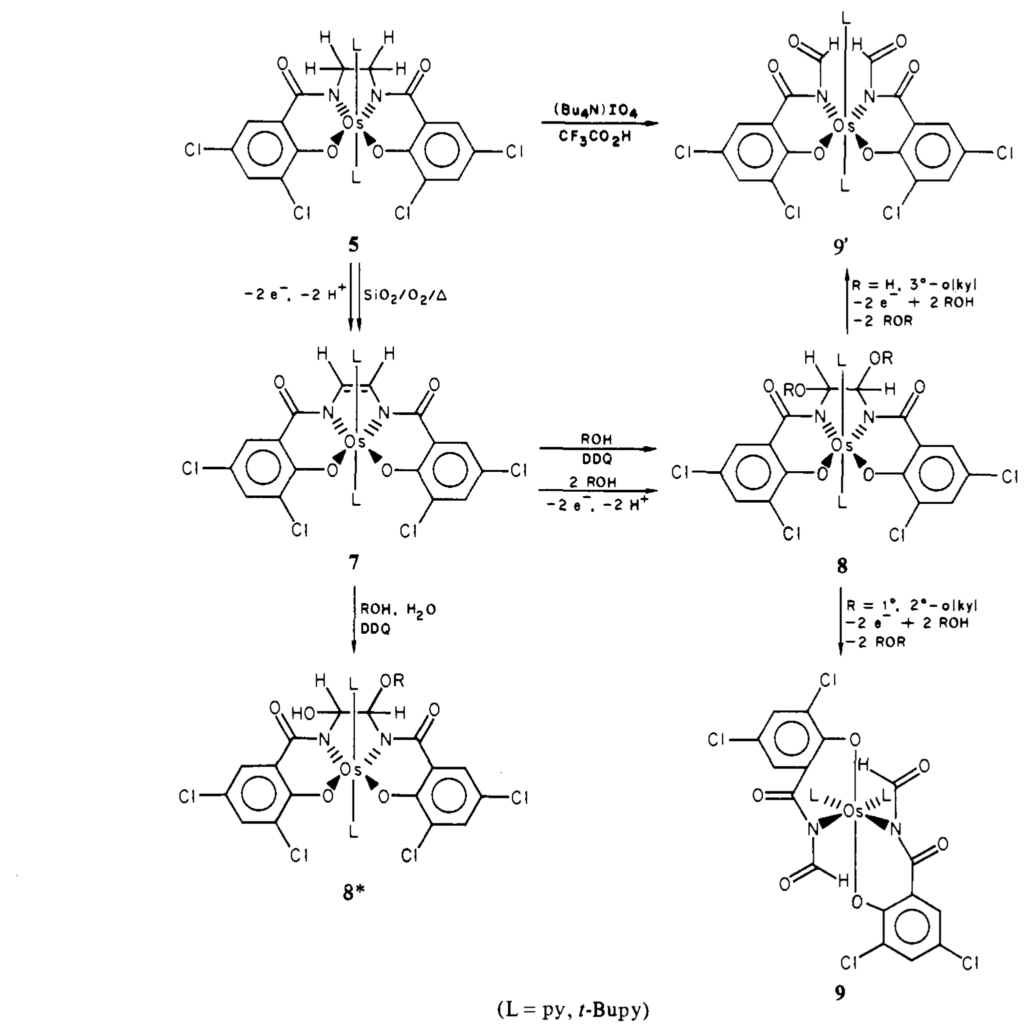

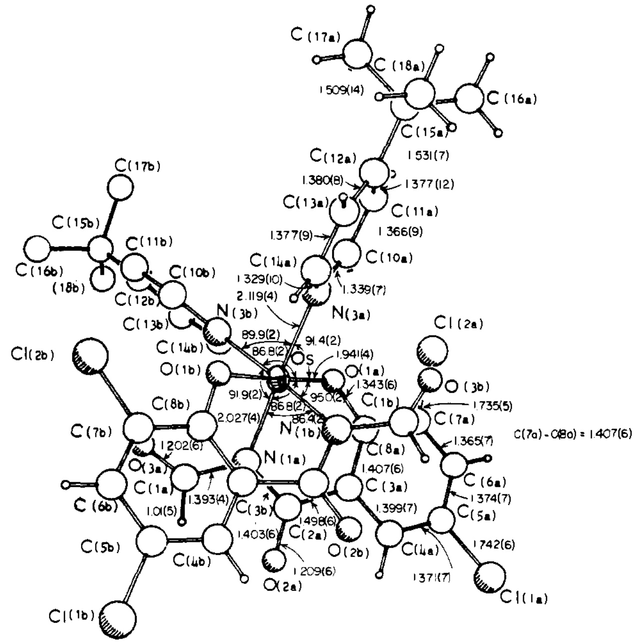

Figure 6. Molecular structure of Os(η^2-Fo-CHBA)$_2$-*cis*-(*t*-Bupy)$_2$ (**9**).

6 is produced in very small concentrations as an intermediate in the electrooxidation of **5**, but not **7**. We have not been able to isolate and characterize this compound.

Chemical conversion of **7** to **8** can be effected in high yield by oxidation with dichlorodicyanobenzoquinone (DDQ) in dichloromethane in the presence of alcohol or water (Scheme II). The five-membered metallacycle in **8** is symmetrically substituted by *trans*-alkoxide groups, but if the oxidation with DDQ is performed in the presence of both alcohol and water the unsymmetrically substituted complex **8*** bearing *trans*-alkoxide and hydroxide groups is produced in addition to the two symmetrical complexes **8** (R = H or alkyl). Complex **8*** forms in very small concentrations in the electrooxidation process when alcohols are used implying the presence of small quantities of water. The structures of these complexes have been confirmed by ^{1}H and ^{13}C NMR (Tables I and II). The ^{1}H NMR spectrum of **8*** shows the multiplicity of signals expected for two inequivalent pyridines and two inequivalent rings in the chelate ligand. For compounds **7** and **8** an alternative structure which would also satisfy the accumulated spectroscopic data involves axial phenoxide ligands with the nitrogen donors in the equatorial plane and the pyridine ligands in a cis configuration. However, this structure would probably be highly strained.

Electrochemical oxidation of **8** at 0.87 V in the presence of alcohol or water results in cleavage of the carbon–carbon bond of the five-membered metallacycle and dealkylation or deprotonation of the oxygen substituents to afford the two diastereomeric complexes **9** and **9′** which differ in cis–trans ligand relationships only. Both complexes with L = *t*-Bupy have been characterized by X-ray crystal structure determinations (see Figure 6 for **9** and Figure 7 for **9′**). These are the first structurally characterized N-coordinated organic imido complexes of osmium. The diastereomeric composition is a function of the R group and the ligand L. For L = py the transformations are 100% stereoselective. When R is methyl, ethyl, *n*-butyl, isopropyl, or benzyl, **9** is the sole product and is formed quantitatively. When R is *tert*-butyl, *tert*-amyl, or H, **9′** is the quantitative product. It was not possible

Scheme III

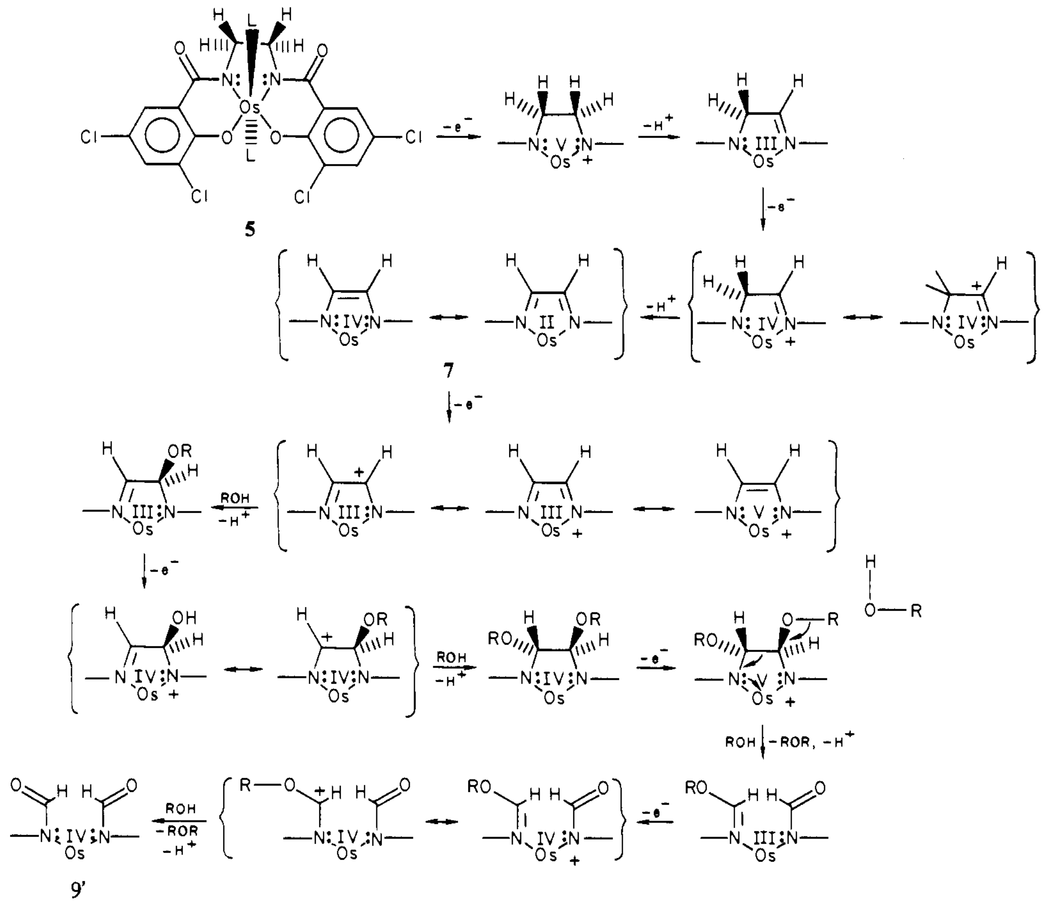

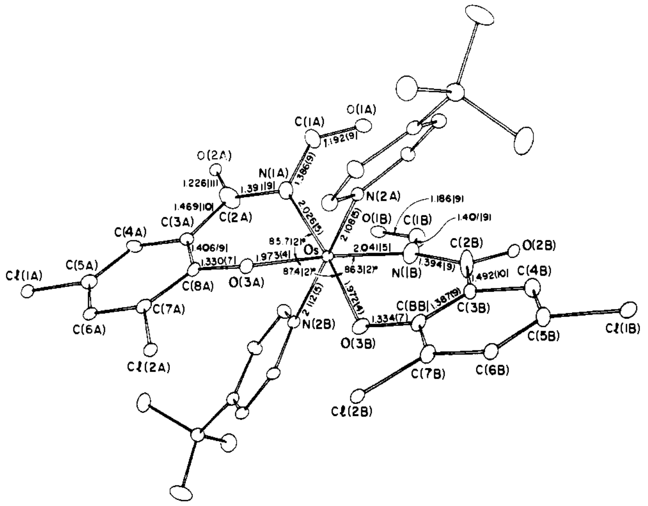

Figure 7. Molecular structure of Os(η^2-Fo-CHBA)$_2$-*trans*-(t-Bupy)$_2$ (9').

to grow crystals suitable for structural analysis with L = py for either diastereomer. Consequently, the entire series of complexes was synthesized with L = t-Bupy. This substitution causes a change in the diastereomeric distribution of 9 and 9'. Thus the electrooxidation of 5 (L = t-Bupy) in the presence of isopropyl alcohol produces a mixture of 9 and 9' in the approximate ratio 7:3. Compound 9' can also be produced as the sole product by oxidation of 5 in dichloromethane with tetrabutylammonium periodate in the presence of excess trifluoroacetic acid (TFA). 9 and 9' have been characterized by NMR (Tables I and II).

At this juncture it might be helpful to suggest a mechanism for the combination of ligand and metal oxidations that we have described (Scheme III). One-electron oxidation of 5 might afford an osmium(V) complex which could undergo spontaneous reductive deprotonation to produce an osmium(III) monoimine complex that would be rapidly oxidized at the potential employed. This would give a cationic osmium(IV) monoimine complex which upon reductive deprotonation would give 7. One-electron oxidation of 7 would produce a complex which possesses carbonium ion character at the carbon atoms of the metallacycle. Nucleophilic attack by alcohol followed by proton loss would lead to another osmium(III) monoimine whose electrooxidation would give 8 by a similar sequence. One-electron oxidation of 8 might induce ring cleavage and O-dealkylation to produce yet another osmium(III) complex whose further oxidation and dealkylation would lead finally to compound 9 or 9'. It is not clear at what stage in the conversion of 8 to 9 the isomerization occurs that gives the observed stereochemistry at the metal center. However, we suspect that isomerization might occur after one-electron oxidation of 8 and that the unusual stereochemistry could be related to the relative rate of this isomerization vs. the rate of ligand oxidation. Evidence presented below demonstrates that an octahedral osmium(IV) complex of ligand 2 can exist with nonplanar tetradentate tetraanionic coordination. Consequently, the isomerization which gives 9 might occur prior to cleavage of the carbon–carbon bond. The stoichiometric conversion of 5 to 9 or 9' would require exactly six electrons according to Scheme III. Experimentally the charge is variable, but it is always greater than or equal to six electrons per osmium atom.

In the presence of acid together with an alcohol or water 9 and 9' undergo two-step quantitative conversions to produce two final new blue complexes. The complexes prepared in this way are effective catalysts for the electrooxidation of alcohols.[16]

These studies demonstrate that it is possible to coordinate 1 as a nonlabile tetradentate tetraanion to osmium and that this type of coordination results in a significant stabilization of higher oxidation states. However, the ethylene unit of 1 is an unsuitable feature for ligands that are designed to resist strongly oxidizing

---

[16] Anson, F. C.; Collins, T. J.; Gipson, S. L.; Krafft, T. E., manuscript in preparation.

Scheme IV

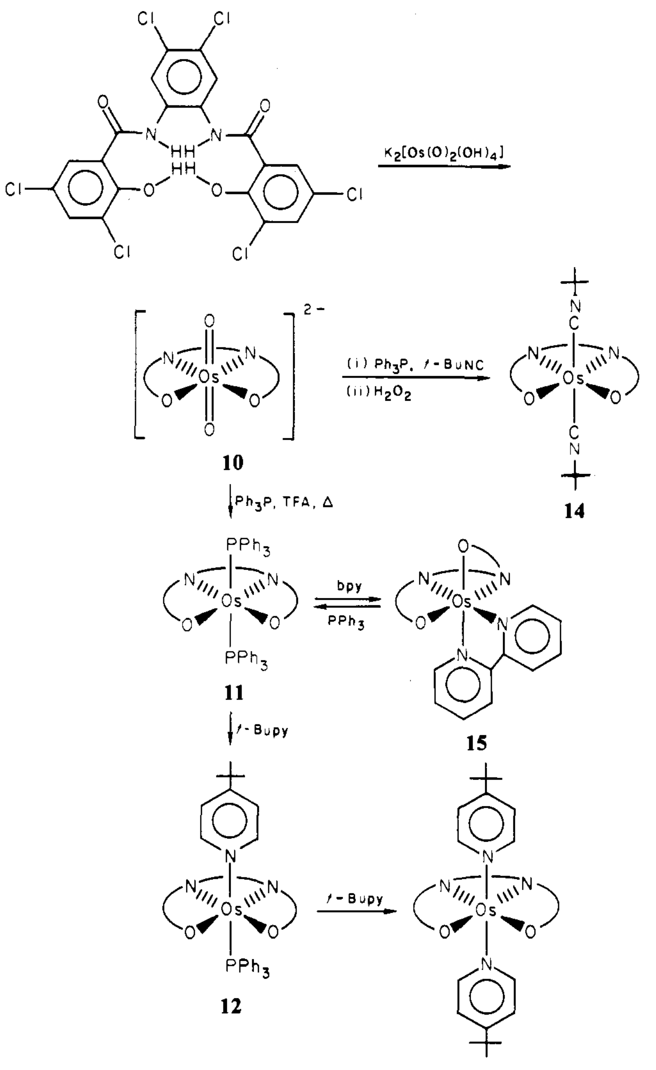

conditions. At the outset of this work it was recognized that the ethylene unit was probably the most easily oxidized portion of **1**, but it was not clear whether the sensitivity would be sufficient to preclude the formation of high oxidation state complexes. The major goal of building stable strongly oxidizing complexes has been achieved in a simple manner by replacing the ethylene unit of **1** with the more oxidation resistant dichlorophenylene bridge of **2**.

Syntheses and Oxidations of Os(IV) Complexes of Ligand 2. Insertion of osmium into ligand **2** and entry into the chemistry of several oxidation states has been accomplished (Scheme IV). The conversion of the osmium(VI) complex $K_2[Os(\eta^4\text{-CHBA-DCB})(O)_2]$ (**10**) to the osmium(IV) complex $Os(\eta^4\text{-CHBA-DCB})(PPh_3)_2$ (**11**) involves the unusual procedure of heating **10** under reflux in a triphenylphosphine/TFA solution. The reaction affords **11** in high yield. Compound **11** is a very versatile intermediate for ligand exchange reactions at osmium(IV), as illustrated in Scheme IV. The compounds shown in Scheme IV have been characterized by ^1H NMR (Table I).

The cyclic voltammogram of $Os(\eta^4\text{-CHBA-DCB})(t\text{-Bupy})_2$ (**13**) is shown in Figure 8. The irreversible response observed upon oxidation of complex **5** (Figure 3) has been converted to a reversible couple at $E^f = +0.70$ V. Bulk electrolysis of dark blue **13** at 1.0 V in dichloromethane consumes one electron per osmium atom and produces a purple solution which apparently contains an equimolar mixture of two osmium(V) complexes. The cyclic voltammogram after electrolysis still contains the original reversible couple arising from **13**, but the peak currents are only about half as large as they were originally. In addition, two new couples appear several hundred millivolts negative and with peak currents also about half as large as the original couples (Figure 9). The open circuit potential of the electrode is positive of all of the couples showing that all of the original osmium(IV) complex has been oxidized. One-electron reduction of the mixture restores a pure solution of **13**. We suspect that the oxidation products are a mixture of geometrical isomers.

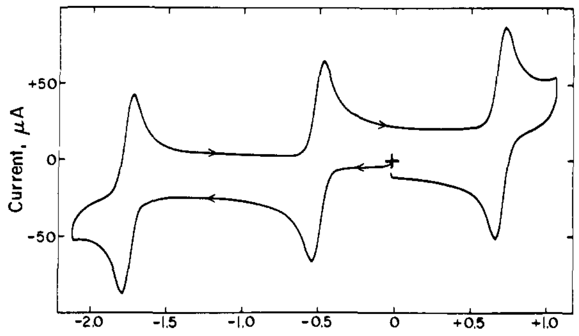

Figure 8. Cyclic voltammogram of 1 mM $Os(\eta^4\text{-CHBA-DCB})(t\text{-Bupy})_2$ (**13**) in CH_2Cl_2, 0.1 M TBAP at 0.174 cm^2 BPG electrode. Scan rate = 200 mV s^{-1}.

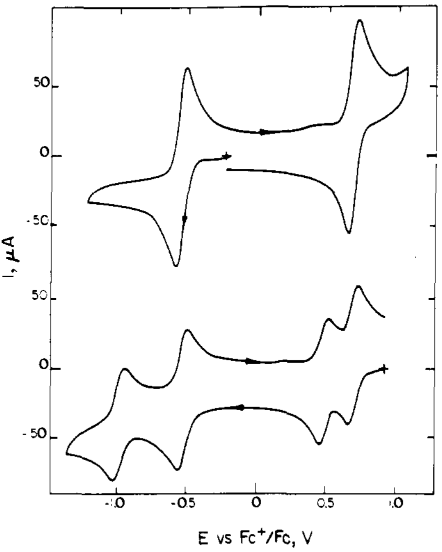

Figure 9. Cyclic voltammogram of (a, top) 1 mM $Os(\eta^4\text{-CHBA-DCB})(t\text{-Bupy})_2$ (**21**) + 0.1 M TBA-BF$_4$ in CH_2Cl_2 and (b, bottom) 1 mM $[Os(\eta^4\text{-CHBA-DCB})(t\text{-Bupy})_2]^+$ + 0.1 M TBA-BF$_4$ in CH_2Cl_2; one-electron reduction restores cyclic voltammogram (a). Pt wire electrode; 200 mV s^{-1}.

A change to nonplanar coordination of the tetradentate tetraanion in **13** upon one-electron oxidation could give rise to an equilibrium mixture of diastereomers. The complex $Os(\eta^4\text{-CHBA-DCB})(PPh_3)_2$ (**11**) which contains *trans*-phosphine ligands might be expected to resist this isomerism since it would require cis coordination of the bulky phosphine ligands. Bulk electrolysis of **11** in acetonitrile at 0.86 V involves one electron per osmium atom and produces a dark green solution of what we assume to be the osmium(V) complex $[Os(\eta^4\text{-CHBA-DCB})(PPh_3)_2]^+$. This oxidized material exhibits no additional waves in the cyclic voltammogram.[17] In order to test the ability of ligand **2** to assume a nonplanar geometry, complex **11** was treated with 2,2′-bipyridine in toluene under reflux and the compound $Os(\eta^4\text{-CHBA-}$

---

[17] For a recent electrochemical study of the systems $[M(bpy)_2(OH_2)_2]^{2+}$ (M = Ru, Os) see: Takeuchi, K. J.; Samuels, G. J.; Gersten, S. W.; Gilbert, J. A.; Meyer, T. J. *Inorg. Chem.* **1983**, *22*, 1407. For the osmium case stable complexes were found for oxidation states II, III, IV, V, and VI with a small variation in $E_{1/2}$ values, Os(III/II) = +0.16 V (SSCE), Os(VI/V) = +0.82 V. Oxidation is accompanied by deprotonation. For a recent electrochemical study of some osmium(IV) and (VI) complexes see: Armstrong, J. E.; Walton, R. A. *Inorg. Chem.* **1983**, *22*, 1545.

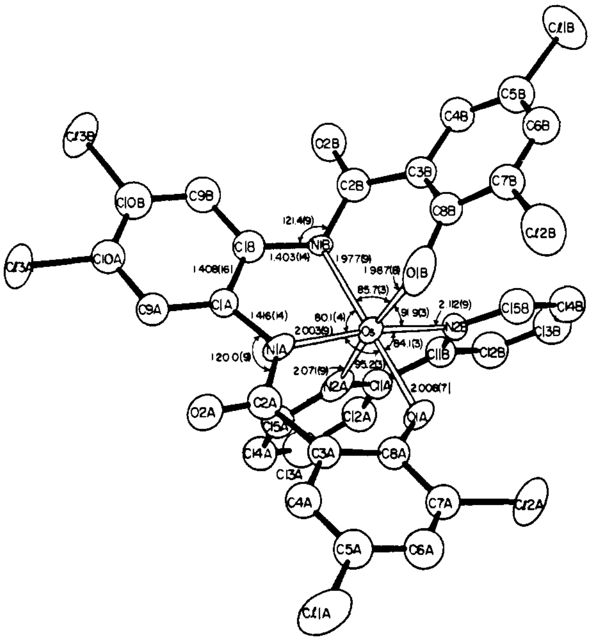

Figure 10. Molecular structure of Os(η^4-CHBA-DCB)(η^2-bpy) (**15**).

DCB)(bpy) (**15**) was isolated from the reaction mixture. X-ray crystal structure analysis of **15** (Figure 10) shows that the bipyridine ligand occupies one axial and one equatorial position of a distorted octahedron with one phenolic donor coordinated axially and the three remaining anionic donors coordinated equatorially. Clearly, under the steric influence of the bipyridine ligand the tetradentate tetraanion can be constrained to coordinate in a nonplanar fashion. We are further investigating these complexes in which the metal is apparently in the rare osmium(V) oxidation state.[18,19]

It is possible to make stable complexes of this type with a number of different axial ligands. By changing the axial ligands we have been able to vary the potential of the osmium(V/IV) couple from +0.59 V to almost +1.00 V. The most potent oxidant generated so far is [Os(η^4-CHBA-DCB)(t-BuNC)$_2$]$^+$ (**14**) with a formal potential for the osmium(V/IV) couple of +0.93 V vs. Fc$^+$/Fc, or ca. 1.65 V vs. NHE.

The results we have presented demonstrate the versatility of ligands such as [η^4-CHBA-Et]$^{4-}$ and [η^4-CHBA-DCB]$^{4-}$ in the formation of both highly oxidizing and highly reducing inorganic complexes. A set of ligand design features that are important in the preparation of stable complexes has been identified. We believe that chelate complexes of this class of ligands will find application in selective redox reactions, and we are actively pursuing such studies with a number of metals and oxidation reactions.

Experimental Section

Materials. All solvents were reagent grade (Aldrich, Baker Mallinckrodt, M.C.B. or U.S.I.) and were used as received unless otherwise noted. Acetic anhydride (reagent, Mallinckrodt), 2-acetylsalicylic acid (Aldrich), 2,2′-bipyridine (99.5%, Aldrich), *tert*-butyl isocyanide (>98%, Fluka), 4-*tert*-butylpyridine (99%, Aldrich), Cl_2 (Matheson), 2,3-dichloro-5,6-dicyano-1,4-benzoquinone (98%, Aldrich), 3,5-dichlorosalicylic acid (Pfaltz and Bauer), glacial acetic acid (Aldrich), $HClO_4$ (60%, Mallinckrodt), H_2O_2 (30% Superoxol, Baker), KOH (reagent, Baker), OsO_4 (99.8%, Alfa), H_2PO_4 (85%, Baker), pyridine (reagent, Mallinckrodt), triethylamine (reagent, M.C.B.), trifluoroacetic acid (reagent, M.C.B.), and triphenylphosphine (99%, Aldrich) were all used as received. The oxalyl chloride and ethylenediamine (Aldrich) used in the ligand syntheses were both freshly distilled. 4,5-Dichloro-*o*-phenylenediamine was dried over Na_2SO_3 and recrystallized from hexane. Silica gel was 60–200 mesh (Davidson). Analytical and preparatory thin layer chromatography plates, 250 and 1000 μm, respectively, were silica gel GF (Analtech). Molecular sieves (4 Å, Linde) were heated under vacuum at 300 °C for 4 h prior to use.

Physical Measurements. ^1H NMR spectra were measured at 90 MHz on a Varian EM 390 or a JEOL FX90-Q spectrometer unless otherwise noted. ^{13}C NMR spectra were measured at 500 MHz on a Bruker WM 500 spectrometer. ^1H and ^{13}C chemical shifts are reported in δ vs. Me_4Si with the solvent ($CDCl_3$ δ 7.25, CD_2Cl_2 δ 5.35, Me_2SO-d_6 δ 2.50 or acetone-d_6 δ 2.05) as internal standard. Infrared spectra were recorded on a Beckman IR 4240 spectrophotometer. Raman data was recorded on a SPEX spectrometer. Elemental analyses were obtained at the Caltech Analytical Facility. Analytical thin layer chromatography results were obtained by elution with CH_2Cl_2/THF (9:1).

Electrochemical Procedures. Dichloromethane (M.C.B. or Mallinckrodt) used in electrochemical experiments was reagent grade and was further purified by passing it over a short column of activated alumina (Woelm N. Akt. I). Acetonitrile (Burdick and Jackson, distilled in glass) was dried over 3-Å molecular sieves. TBAP supporting electrolyte (Southwestern Analytical Chemicals) was dried, recrystallized twice from acetone/ether, and then dried under vacuum. The TBAP concentration in all solutions was 0.1 M. Alcohols were reagent or spectrophotometric grade and were used as received. BPG electrodes (Union Carbide Co., Chicago) used for cyclic voltammetry were cut and mounted as previously described.[20] The BPG electrode used for controlled potential oxidations was cut as a thin sheet (~1.7 × 4.5 × 0.07 cm) from a rectangular block. The reference electrodes used were a saturated KCl silver–silver chloride electrode (Ag/AgCl), a saturated sodium chloride calomel electrode, and a silver wire quasireference electrode. In all cases ferrocene was added at the conclusion of the experiment as an internal potential standard. All potentials are quoted with respect to the formal potential of the ferrocinium/ferrocene couple, which under these conditions we have consistently measured as +0.48 V vs. SCE, or ca. 0.70 V vs. NHE.

Cyclic voltammetry and controlled potential electrolysis were performed on a Princeton Applied Research Model 173/179 potentiostat/digital coulometer equipped with positive feedback IR-compensation and a Model 175 universal programmer. Current–voltage curves were recorded on a Houston Instruments Model 2000 X–Y recorder. Standard two- and three-compartment electrochemical cells were used. Controlled potential oxidations in dichloromethane in the presence of water or alcohol were conducted at a BPG anode with the Ag/AgCl reference electrode placed in the anolyte solution near the anode to reduce the amount of IR-compensation needed. Controlled potential electrolyses in acetonitrile were conducted at a Pt gauze working electrode with the reference electrode isolated in a separate compartment. These experiments were performed in a helium atmosphere dry box (Vacuum/Atmospheres Co.).

X-ray Data Collection and Structure Determination of 5. A suitable crystal was obtained by slow crystallization from THF/water. Oscillation and Weissenberg photographs showed symmetry no higher than $\bar{1}$. The intensity data were collected on a locally modified Syntex $P2_1$ diffractometer with graphite monochromator and Mo K$\bar{\alpha}$ radiation (λ 0.7107 Å). Unit cell parameters (Table IV) from least-squares refinement of $\sin^2\theta$ based on fifteen 2θ values, each 2θ an average of four values ($\pm 2\theta$, $\pm\omega$, φ, χ; $\pm 2\theta$, $\pm\omega$, $\pi + \varphi$, $\pi - \chi$). The three check reflections indicated no decomposition and the data were reduced to F_o^2; the variances of the intensities were obtained from counting statistics with an additional term (0.02 × scan counts).[2] The form factors were taken from ref 21.

The Os atom coordinates were derived from a Patterson map, and successive electron density maps revealed the remaining atoms. Hydrogen atoms were introduced into the model at idealized positions with fixed $U = 0.063$ Å^2. Several cycles of least-squares refinement, minimizing $\sum w\Delta^2$, with $w = \sigma^{-2}(F_o^2)$ and $\Delta = F_o^2 - (F_c/k)^2$, resulted in $S = 1.92$ and $R_F = 0.034$.[22] The final value for the isotropic extinction coefficient was 0.396 (36) × 10^{-6}. The calculations were carried out on a Vax 11/780 with the CRYM system of programs.[23]

X-ray Data Collection and Structure Determination of 9. A long crystal of **9** (L = t-Bupy) was obtained by slow crystallization from CH_2Cl_2/hexane. Diffractometer data (Nicolet diffractometer, graphite monochromator, Mo Kα radiation) indicated monoclinic symmetry and space group $C2/c$ (Table IV). The six check reflections indicated no decomposition, and following an empirical correction for absorption, the data were reduced to F_o^2.

---

(18) "Gmelin Handbuch der Anorganischen Chemie"; Osmium Supplement; Springer-Verlag: New York, 1980; Vol. 1.

(19) Cotton, F. A.; Wilkinson, G. "Advanced Inorganic Chemistry"; 4th ed.; John Wiley and Sons: New York, 1980; pp 912–933.

(20) Oyama, N.; Anson, F. C. *J. Am. Chem. Soc.* **1979**, *101*, 3450.

(21) Atomic scattering factors were taken from: "International Tables for X-ray Crystallography"; Witton: Birmingham, 1974; Vol. IV, pp 72–97.

(22) The goodness-of-fit $S = [\sum w\Delta^2/n - v)]^{1/2}$, n = number of reflections, v = number of parameters; $R_F = \sum|\Delta F|/\sum|F_o|$ (based on reflections with $I > 0$), $\Delta F = |F_o| - |F_c|$, $R_{F'} = R_F$ (based on reflections with $I > 3\sigma_I$).

(23) The CRYM computing system was used (D. J. Duchamp, California Institute of Technology).

Table I. 90-MHz ^{1}NMR Data for All Osmium Complexes[a]

		chelate ligand			pyridine				other	
no.	compd	H_1	H_2, H_3[b]		H_o	H_m	H_p	*t*-Bu		
1[c]	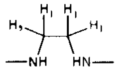	3.70 s, 4	7.54 d, 2	7.74 d, 2						
3[d]		3.88 s, 4	7.27 d, 2	8.21 d, 2					3.77 s, 2 } H_2O	
5[e]	L = py	68.55 s, 4	10.55 d, 2	14.93 d, 2	−6.29, d, 4 $J_{o,m}$ = 8 Hz	7.73, dd, 4 $J_{m,o}$ = 8 Hz $J_{m,p}$ = 8 Hz	−1.39, t, 2 $J_{p,m}$ = 8 Hz			
5[e]	L = *t*-Bupy	69.78 s, 4	10.78 d, 2	15.40 d, 2	−7.26, d, 4 $J_{o,m}$ = 7.5 Hz	7.38, d, 4 $J_{m,o}$ = 7.5 Hz		0.18 s, 18		
7[e]	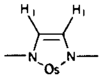	−15.52 s, 2	4.26 d, 2	5.38 d, 2	−1.12, d, 4 $J_{o,m}$ = 8 Hz	7.38, dd, 4 $J_{m,o}$ = 8 Hz $J_{m,p}$ = 8 Hz	−2.29, t, 2 $J_{p,m}$ = 8 Hz			
7[e]	L = *t*-Bupy	−14.30 s, 2	4.89 d, 2	5.61 d, 2	−2.90, d, 4 $J_{o,m}$ = 7.5 Hz	7.11, d, 4 $J_{m,o}$ = 7.5 Hz		0.13 s, 18		
8a[e,f]	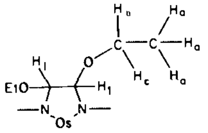	6.01 s, 2	9.22 d, 2	10.48 d, 2	−1.32, dd, 4 $J_{o,m}$ = 7.5 Hz $J_{o,p}$ = 1.5 Hz	8.59, dd, 4 $J_{m,p}$ = 8.5 Hz $J_{m,o}$ = 7.5 Hz	1.61, tt, 2 $J_{p,m}$ = 8.5 Hz $J_{p,o}$ = 1.5 Hz		2.06, dd, 6 $J_{a,b} = J_{a,c}$ = 8 Hz } H_a 7.54, dq, 2 $J_{a,b}$ = 8 Hz $J_{b,c}$ = 10 Hz } H_c H_b	6.08, dq, 2 $J_{a,c}$ = 8 Hz $J_{c,b}$ = 10 Hz } H_b H_c
8b[e]	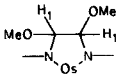	6.77 s, 2	9.43 d, 2	10.91 d, 2	−1.75, d, 4 $J_{o,m}$ = 7.5 Hz	8.60, dd, 4 $J_{m,o}$ = 7.5 Hz $J_{m,p}$ = 7.5 Hz	1.25, t, 2 $J_{p,m}$ = 7.5 Hz		5.77 s, 6 } $-CH_3$	
8*[e,g]	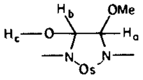		14.43 d, 1 10.67 d, 1	12.79 d, 1 10.29 d, 1	−2.59, dd, 2 $J_{o,m}$ = 7.5 Hz $J_{o,p}$ = 1.5 Hz −6.85, dd, 2 $J_{o,m}$ = 7.5 Hz $J_{o,p}$ = 1.5 Hz	8.94, dd, 2 $J_{m,p}$ = 8.5 Hz $J_{m,o}$ = 7.5 Hz 7.83, dd, 2 $J_{m,p}$ = 8.5 Hz $J_{m,o}$ = 7.5 Hz	−0.57, tt, 1 $J_{p,m}$ = 8.5 Hz $J_{p,o}$ = 1.5 Hz −1.00, tt, 1 $J_{p,m}$ = 8.5 Hz $J_{p,o}$ = 1.5 Hz		4.87 s, 3 } $-CH_3$ 8.59 s, 1 } H_a	16.87, d, 1 $J_{c,d}$ = 3 Hz } H_b 7.57, d, 1 $J_{d,c}$ = 3 Hz } H_c
9[e]	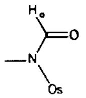 L = *t*-Bupy		7.65 d, 2	9.52 d, 2	5.33, d, 4 $J_{o,m}$ = 7.5 Hz	9.67, d, 4 $J_{m,o}$ = 7.5 Hz		1.67 s, 18	10.44 s, 2 } H_a	
9′[e]	L = py		7.39 d, 2	8.11 d, 2	5.23, d, 4 $J_{o,m}$ = 8 Hz	9.20, dd, 4 $J_{m,o}$ = 8 Hz $J_{m,p}$ = 8 Hz	6.26, t, 2 $J_{p,m}$ = 8 Hz		7.28 s, 2 } H_a	
9′[e]	L = *t*-Bupy		7.30 d, 2	7.96 d, 2	4.92, d, 4 $J_{o,m}$ = 7.5 Hz	9.08, d, 4 $J_{m,o}$ = 7.5 Hz		1.42 s, 18	7.14 s, 2 } H_a	
2[h]	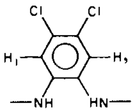	8.12 s, 2	7.87 d, 2	8.10 d, 2						

Table I (*Continued*)

10[c]	9.47 s, 2	7.40 d, 2	8.39 d, 2					
11[e]	4.54 s, 2	8.39 d, 2	9.33 d, 2				8.05, m, 12} H_o 6.95, dd, 12 $J_{m,o} = J_{m,p} = 8$ Hz} H_m	7.42, t, 6 $J_{p,m} = 8$ Hz} H_p
12[i]	5.60 s, 2	9.31 d, 2	11.64 d, 2	−2.66, d, 2 $J_{o,m} = 6$ Hz	7.48, d, 2 $J_{m,o} = 6$ Hz	0.30 s, 9	9.13, dd, 6 $J_{P\text{-}H_o} = 13$ Hz $J_{o,m} = 8$ Hz} H_o	7.29, dd, 6 $J_{m,o} = J_{m,p} = 8$ Hz} H_m 7.68, t, 3 $J_{p,m} = 8$ Hz H_p
13[i]	7.50 s, 2	9.78 d, 2	11.10 d, 2	−8.48, d, 4 $J_{o,m} = 7$ Hz	7.96, d, 4 $J_{m,o} = 7$ Hz	0.07 s, 18		
14[e]	8.39 s, 2	7.43 d, 2	8.42 d, 2				1.44 s, 18} t-BuNC	
15[e]	8.28 s, 2	7.11 d, 2	8.20 d, 2				8.58, d 2 $J = 8$ Hz 7.76, d, 2 $J = 8$ Hz} bpy	7.54, dd, 2 $J = 8$ Hz 7.94, dd, 2 $J = 8$ Hz} bpy

[a] The chemical shifts of the paramagnetic Os(IV) species are somewhat concentration dependent. The values reported here are uncorrected. [b] $J_{2,3} = J_{3,2} = 3$ Hz. [c] δ in acetone-d_6. [d] δ in D_2O. [e] δ in $CDCl_3$. [f] Selective ^1H decoupling experiments have confirmed these assignments. [g] H_d readily exchanges on addition of D_2O which causes collapse of the H_c signal to a singlet. [h] δ in $(CD_3)_2SO$. [i] δ in CD_2Cl_2.

Table II. Selected 500-MHz ^{13}C NMR Data

no.	compd	C_1 (proton coupled)	C_1 (H_1 or H_a selectively decoupled)
7[a]	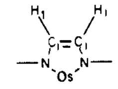	105.28, d_1 $J_{CH} = 187$ Hz	105.28, s
8a[a]	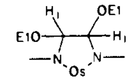	51.76, d $J_{CH} = 160$ Hz	51.76, s
9[a]	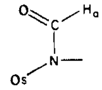 L = t-Bupy	196.46, d $J_{CH} = 208$ Hz	196.46, s

[a] δ in $CDCl_3$.

Table III. Formal Potentials of Os Compounds

compd	III/II[a]	IV/III[a]	V/IV[a,b]
5	−1.88	−0.65	(+0.70)
5, L = t-Bupy	−1.96	−0.70	(+0.66)
7	−1.76	−0.62	+0.37[c]
8b	−1.95	−0.64	(ca. +0.9)
9	−1.88	−0.46	*d*
9′	−1.88	−0.39	*d*
11	−1.72	−0.46	+0.59
13	−1.77	−0.51	+0.70
14	−1.05	−0.57	+0.92

[a] Potentials were measured against the Fc^+/Fc couple which we have measured at ca. 0.48 V vs. SCE. [b] Potentials in parentheses are peak potentials of irreversible oxidations. [c] **7** also exhibits an irreversible oxidation at +0.92 V. [d] No oxidations seen at potentials below +1.1 V.

Solution of the structure was by the Patterson map, and refinement was on $|F|$. The solvent molecule, CH_2Cl_2, is disordered, and attempts to model it and refine the remainder of the structure gave $R_F = 0.031$ and $S' = [\sum w(\Delta F)^2/\sum wF_o^2]^{1/2} = 1.60$; final average shift/error = 0.02, the maximum deviation in final ΔP map is 0.59 e/Å^3. The data collection and refinement was carried out by Crystalytics Co.

X-ray Data Collection and Structure Determination of 9′. A thin needlelike crystal of **9′** (L = t-Bupy) was obtained from a solution of CH_2Cl_2/EtOH. Oscillation and Weissenberg photographs showed symmetry no higher than $\bar{1}$. The unit cell parameters (Table IV) were determined from a refinement using fifteen 2θ values with $25° < |2\theta| < 35°$, averaged from centered values at both $+2\theta$ and -2θ. The intensity data were collected on a locally modified Syntex $P2_1$ diffractometer with graphite monochromator and Mo Kα radiation. The three check reflections indicated no decomposition, and the data were reduced to F_o^2 as above. The form factors of Os and Cl were corrected for anomalous dispersion.

Solution and refinement of the structure proceeded smoothly; the position of the Os atom was derived from the Patterson map, and the Fourier map phased on the Os atom revealed the remainder of the structure. The H atoms were introduced into the model with fixed coordinates at idealized positions (the methyl H atoms from ΔF maps) and fixed Gaussian amplitudes of $U = 0.10$ Å^2—full-matrix least-squares refinement of the non-H atoms with anisotropic U_{ij}'s with use of all reflections with $I > 0$;[22] final average shift/error = 0.04 in the last cycle, and the maximum deviation in the final $\Delta\rho$ map of 2.5 e/Å^3.

X-ray Data Collection and Structure Determination of 15. A crystal of **15** was obtained from a solution of CH_2Cl_2/EtOH. Oscillation and Weissenberg photographs indicated that the space group was triclinic. A hemisphere of intensity data were collected as above with unit cell parameters obtained by least-squares refinement of the orientation matrix with use of fifteen reflections in the range $10.9 < 2\theta < 19.8°$ (Table IV) with positive 2θ measurements only. The three check reflections, remeasured after every 100 reflections, indicated no significant decay over the 89 h of data collection. Absorption corrections were deemed unnecessary. The data were reduced to F_o^2 as above,[10] with anomalous dispersion corrections included for Os. The atomic position of the Os atom was derived from the Patterson map. Subsequent Fourier and difference maps revealed all non-hydrogen atoms.

Several cycles of full-matrix least-squares refinement on all non-hydrogen parameters yielded $R_F = 0.047$, $R_F' = 0.044$, and GOF = 3.44;[22] final shift/errors < 0.10; and a data-to-parameter ratio = 11.0. All atomic coordinates as well as the scale factor, *k*, and Gaussian ellipsoids

Table IV. Summary of Data Collection and Refinement Information

	5	**9**	**9′**	**15**
formula	$C_{26}H_{18}OsN_4O_4Cl_4$	$C_{34}H_{32}OsN_4O_6Cl_4{\cdot}CH_2Cl_2$	$C_{34}H_{32}OsN_4O_6Cl_4$	$C_{30}H_{14}OsN_4O_4Cl_6{\cdot}{}^1/{}_2C_2H_6O$
formula wt	782.47	1009.60	924.67	920.42
space group	$P\bar{1}$	$C2/c$	$P\bar{1}$	$P\bar{1}$
a, Å	10.083 (4)	19.907(6)	8.5333 (9)	10.860 (3)
b, Å	12.310 (5)	28.850 (7)	13.6879 (19)	12.633 (3)
c, Å	12.241 (4)	9.445 (3)	16.4148 (18)	12.844 (4)
σ, deg	97.38 (3)	90	104.350 (13)	117.47 (2)
β, deg	96.49 (4)	131.79 (2)	97.329 (11)	90.42 (3)
γ, deg	113.0 (3)	90	79.179 (12)	95.90 (2)
v, A^3	1364.7 (9)	4044 (2)	1817.8 (4)	1552.2 (7)
Z	2	4	2	2
D_{calcd}, g cm^{-3}	1.90	1.66	1.69	1.97
crystal size, mm	0.14 × 0.19 × 0.92	0.11 × 0.20 × 0.80	0.10 × 0.23 × 0.42	0.24 × 0.27 × 0.30
λ, Å	0.7107	0.7107	0.7107	0.7107
μ, mm^{-1}	5.11	3.60	3.86	4.68
scan type	θ–2θ	ω	θ–2θ	θ–2θ
2θ limits	$3 < 2\theta < 60°$	3–43°, 43–55°	4–30°, 25–56°	$4 < 2\theta < 40°$
scan rate, deg/min	2	6, 4	6, 2	2
scan width, deg	2.4	0.9	2.0	2.0
total collected refl	12429		9710	3283
final refl	6630	4657	8315	2915
refinement on	F^2	F	F^2	F^2
sec. extinction	3.9 (4) × 10^{-7}	5 × 10^{-5}		
final no. of parameters	353	264	442	264
final cycle [a]				
R_F	0.034 (6435)		0.051 (7989)	0.047 (2888)
R'_F	0.029 (5805)	0.031 (3903)	0.043 (6871)	0.044 (2710)
S	1.92 (6630)	1.60 (3903)	2.16 (8315)	3.44 (2915)

[a] The number of reflections contributing to sums given in parentheses; see ref 22 for definitions.

(anisotropic for all atoms except carbon and hydrogen) were in one block.

A difference map calculated after all non-hydrogen atoms have been located revealed the presence of additional electron density near a center of symmetry. This was measured to be an ethanol molecule with the two carbon atoms related by the center of symmetry and the two oxygen atoms disordered over two sites.

Hydrogen atoms were placed at a distance of 0.95 Å from their respective carbon or oxygen atoms by assuming ideal geometry and were not refined. The hydrogen atom temperature factors were set equal to the temperature factor of the atom to which they were attached.

Syntheses. All reactions were carried out in air unless otherwise noted. $K_2[Os(OH)_4(O)_2]$[24] and 3,5-dichloroacetylsalicylic acid[25] were prepared as described in the literature.

H_4CHBA-Et (1).[5] A 250-mL round-bottom flask with a stir bar was charged with 50.0 g (0.277 mol) of 2-acetylsalicylic acid and 50–60 mL of neat oxalyl chloride. The reaction flask was vented to a hood and maintained at 30 °C for 4 h. The remaining oxalyl chloride was distilled off in vacuo. The residue was dissolved in a 30-mL aliquot of CH_2Cl_2 which was also distilled off in vacuo; this step was repeated several times. A 500-mL round-bottom flask, equipped with a stir bar, was charged with a solution of 9.28 mL (0.138 mol) of ethylenediamine in 100 mL of CH_2Cl_2 and immersed in an ice bath. The acid chloride residue was dissolved in 100 mL of CH_2Cl_2, transferred to a dripping funnel and slowly added to the ethylenediamine solution with rapid stirring. The resulting slurry was stirred for 1 h. An excess of 1 equiv of triethylamine was added and the mixture stirred for an additional 0.5 h. This mixture was treated with ca. 100 mL of 6 M NaOH and heated in vacuo to remove the organic volatiles. The remaining aqueous solution was decanted from the undissolved organic residues which were then dissolved in a minimal amount of acetone and retreated with 6 M NaOH solution. All aqueous portions were combined and cautiously acidified with concentrated HCl. The precipitate was collected, washed with water, and recrystallized from acetone/water: yield 33.3 g (80%). Chlorination proceeded as follows: The unchlorinated product (5.0 g) was dissolved in 80–100 mL of glacial acetic acid in a 500-mL filtration flask. Chlorine gas was bubbled through the stirred solution for 0.5 h. The precipitated product was collected, washed with water, and recrystallized from acetone/water: yield 6.6 g (90%); ^{1}H NMR (Table I). Anal. Calcd for $C_{16}H_{12}Cl_4N_2O_4$: C, 43.87; H, 2.76; Cl, 32.37; N, 6.39. Found: C, 44.01; H, 2.81; Cl, 32.59; N, 6.36.

H_4CHBA-DCB (2).[5] 3,5-Dichloroacetylsalicylic acid (12.55 g, 50.39 mmol) was converted to the acid chloride with 10–15 mL of neat oxalyl chloride according to the procedure described for **1**. 4,5-Dichloro-*o*-phenylenediamine (3.78 g, 21.35 mmol) was dissolved in 100 mL of CH_2Cl_2 and 15 mL of THF and cooled to 0 °C. The acid chloride was dissolved in 50 mL of CH_2Cl_2 and slowly added to the diamine solution. After the mixture was stirred for 1 h at 0 °C an excess of 1 equiv (12 mL) of triethylamine was added and the solution stirred for an additional 0.5 h at room temperature. This mixture was then treated with ca. 200 mL of 1 M NaOH and heated in vacuo to remove the organic volatiles. Ethanol was added to the resulting mixture until it became homogeneous. The solution was then slowly acidified with 1 M $HClO_4$. The precipitate was collected, washed with water, and recrystallized from THF/ethanol: yield 7.28 g (61%); ^{1}H NMR (Table I). Anal. Calcd for $C_{20}H_{10}Cl_6N_2O_4$: C, 43.28; H, 1.82; N, 5.05. Found: C, 43.34; H, 1.95; N, 5.00.

$K_2[Os(\eta^4$-CHBA-Et)$(O)_2]{\cdot}H_2O$ (3). Addition of a blue methanol solution of $K_2[Os(OH)_4(OH)_2]$ (0.500 g in 100 mL) to a colorless acetone solution containing 1 equiv of pure H_4CHBA-Et (0.595 g in 80 mL) produced an immediate color change to deep orange. The solution was stirred at room temperature for 10 min and then evaporated to dryness to give a quantitative yield of the product. Recrystallization of 200 mg from acetone/CH_2Cl_2 yielded 179 mg (90%) of orange microcrystalline product. After the sample was heated at 80 °C for 12 h under vacuum, NMR showed the presence of one H_2O per molecule of complex. On standing in air the compound reabsorbs ca. 3 additional molecules of H_2O per molecule of complex: Raman (aqueous) 870 cm^{-1} ($\nu_s(OsO_2)$); IR (Nujol) 820 cm^{-1} (v s, $\nu_{as}(OsO_2)$); ^{1}H NMR (Table I). Anal. Calcd for $C_{16}H_8Cl_4K_2N_2O_6Os{\cdot}(H_2O)$: C, 25.54; H, 1.34; N, 3.72. Found: C, 25.44; H, 1.50; N, 3.61. Incorporation of ^{18}O was effected by letting the compound stand with $H_2{}^{18}O$ for 24 h: IR (Nujol) 788 cm^{-1} (v s, $\nu_{as}(Os^{18}O_2)$).

$Os(\eta^4$-CHBA-Et)$(py)_2$ (5). $K_2[Os(\eta^4$-CHBA-Et)$(O)_2]{\cdot}(H_2O)_4$ (**3**) (0.540 g) was dissolved in 20 mL of pyridine and 15 mL of H_2O. Two equivalents of triphenylphosphine (0.356 g) in 15 mL of pyridine were added and the mixture was heated with stirring at 60 °C for 0.5 h. The reaction was accompanied by a color change to deep red-orange. The solution was evaporated to dryness and the residue warmed under vacuum for an additional 12 h to ensure complete removal of the solvents. The dry residue was washed with 20 mL of CH_2Cl_2 to remove the phosphines. The reduced intermediate, **4**, was collected as a red-brown solid which was then redissolved in 50 mL of THF and 10 mL of H_2O. To this solution was added 30% H_2O_2 (ca. 20 mL) in 20 mL of THF while cooling in a 0 °C bath. The solution was stirred at room temperature for ca. 15 min or until the color change to deep royal blue was complete. Addition of 20 mL of methanol followed by slow removal of the THF yielded 0.405 g (77% based on **3**) of the deep blue crystalline product. An analytical sample was obtained by slow crystallization from THF/hexane: ^{1}H NMR (Figure 2) (Table I). Anal. Calcd for $C_{26}H_{18}Cl_4N_4O_4Os$: C, 39.91; H, 2.32; N, 7.16. Found: C, 39.93; H, 2.42; N, 7.14.

---

(24) Malin, J. M. *Inorg. Synth.* **1980**, *20*, 61.

(25) Durst, H. D.; Gokel, G. W. "Experimental Organic Chemistry"; McGraw-Hill: New York, 1980; p 256.

Os(η^4-CHBA-ethylene)(py)$_2$ (7).[5] Os(η^4-CHBA-Et)(py)$_2$ (5) (100 mg) was dissolved in 50 mL of THF and placed in a 250-mL round-bottom flask with 15 g of silica gel. The mixture was stirred and heated at reflux for 1 h and then evaporated to dryness. The dry silica was heated at 120 °C for 1 h and then placed on top of a small quantity of clean silica gel in a short column. Elution with CH_2Cl_2/acetone (4:1) removed the bulk of the product as a bright yellow band. Some starting material, **5**, and what appeared to be some of the corresponding Os(III) salt, **4**, remained on the column. Second and third fractions of the product were obtained by again heating the dry silica at 120 °C for 1 h and eluting on a short column as before. Filtration and removal of solvent from the combined fractions yielded the product as a dark gold-brown microcrystalline solid in >90% yield. An analytical sample was obtained by recrystallization from $CHCl_3$/hexane: ^1H and ^{13}C NMR (Tables I and II) (Figure 4). Anal. Calcd for $C_{26}H_{16}Cl_4N_4O_4Os$: C, 40.01; H, 2.07; N, 7.18. Found: C, 39.93; H, 2.10; N, 7.18.

Os(η^4-CHBA-*t*-1,2-diEtO-Et)(py)$_2$ (8a).[5] Os(η^4-CHBA-ethylene)(py)$_2$ (7) (100 mg) was dissolved in 20 mL of absolute ethanol and 20 mL of CH_2Cl_2. Addition of 90 mg of dichlorodicyanobenzoquinone (DDQ) caused an immediate color change to deep royal blue. After removal of the solvents by evaporation the product was extracted into CH_2Cl_2 and purified on a short silica gel column by elution with CH_2Cl_2/acetone (9:1). After recrystallization from CH_2Cl_2/pentane the product was obtained as a dark blue microcrystalline solid: yield 76 mg (68%); ^1H and ^{13}C NMR (Tables I and II). Anal. Calcd for $C_{30}H_{26}Cl_4N_4O_6Os$: C, 41.39; H, 3.01; N, 6.44. Found: C, 41.23; H, 2.96; N, 6.43.

Os(η^4-CHBA-*t*-1,2-diMeO-Et)(py)$_2$ (8b).[5] Os(η^4-CHBA-ethylene)(py)$_2$ (7) (100 mg) was dissolved in 20 mL of absolute methanol and 20 mL of CH_2Cl_2. The solution was treated with DDQ as for **8a** and the crude product was purified on two successive short silica gel columns. Recrystallization from CH_2Cl_2/pentane yielded the product as a dark blue powder. NMR established the structure of the product but also showed the presence of a small impurity (<10%). The impurity was separated from the product on a preparatory thin layer chromatography plate with CH_2Cl_2/THF (5:1). ^1H NMR indicated that the impurity was an asymmetrically substituted compound with one hydroxy and one methoxy group on the ligand bridge. This compound, **8***, was the first in this series that had inequivalent NMR signals for the two pyridine ligands and for the two aromatic rings in the chelating ligand. It was therefore deliberately synthesized as discussed below. After removal of the impurity, the major product, **8b**, was again recrystallized from CH_2Cl_2/pentane: yield 43 mg (40%); ^1H NMR (Table I). Anal. Calcd for $C_{28}H_{22}Cl_4N_4O_6Os$: C, 39.92; H, 2.63; N, 6.65. Found: C, 39.94; H, 2.69; N, 6.61.

Os(η^4-CHBA-*t*-1-OH-2-MeO-Et)(py)$_2$ (8*).[5] Os(η^4-CHBA-ethylene)(py)$_2$ (7) (100 mg) was dissolved in 24 mL of CH_2Cl_2, 18 mL of absolute methanol and 3 mL of H_2O. The solution was oxidized with DDQ as for **8a** and **8b**. The reaction mixture was washed down a short silica gel column to separate out the quinones. TLC indicated that the crude product contained three blue compounds in the approximate ratio of 1:2:1. The three were separated on a preparatory thin layer chromatography plate with CH_2Cl_2/THF (4:1). One of the minor components was shown by NMR to be the dimethoxy-substituted compound **8b**. The major component proved to be the desired product, **8***, and the other minor component was presumably the dihydroxy-substituted compound. The product was recrystallized from CH_2Cl_2/pentane and obtained as a dark blue microcrystalline solid: yield 35 mg (33%); ^1H NMR (Table I). Anal. Calcd for $C_{27}H_{20}Cl_4N_4O_6Os$: C, 39.14; H, 2.43; N, 6.76. Found: C, 38.97; H, 2.56; N, 6.55.

Os(η^2-Fo-CHBA)$_2$-*cis*-(py)$_2$ (9).[5] **Method a.** Os(η^4-CHBA-Et)(py)$_2$, (40 mg, 0.051 mmol) was dissolved in 25 mL of CH_2Cl_2 containing 0.1 M TBAP and 1 M of a 1° or 2° alcohol (methanol, *n*-butyl alcohol, isopropyl alcohol, or benzyl alcohol). The solution was electrolyzed in a three-compartment electrochemical cell at a BPG anode at +1.40 V vs. Ag/AgCl until the current had decayed to <5% of its initial value and TLC indicated that the reaction was complete. The anolyte was transferred to a beaker, and 65 mL of ether was slowly added. The precipitated TBAP was removed by filtration, and the solvents were evaporated from the filtrate. The resulting oil was dissolved in 25 mL of acetone, and the product was precipitated by addition of 50 mL of H_2O. The dark blue product was redissolved in CH_2Cl_2, dried over $MgSO_4$, and precipitated with hexane: yield 30 mg (72%). Anal. Calcd for $C_{26}H_{16}Cl_4N_4O_6Os$: C, 38.44; H, 1.99; N, 6.90. Found: C, 38.41; H, 2.06; N, 6.88.

Method b. Os(η^4-CHBA-ethylene)(py)$_2$ (7) (8 mg) was dissolved in 10 mL of CH_2Cl_2 containing 0.1 M TBAP and 0.5 M isopropyl alcohol. The solution was electrolyzed according to the procedure described in method a to give the desired product, **9**, and a trace of **9′**.

Several experiments were performed in which **9** was prepared from 1 mM **5** and 0.5 M benzyl alcohol and the product solution was analyzed by HPLC for benzyl ether. The HPLC analyses were performed on an IBM LC/9533 ternary gradient liquid chromatograph equipped with an octadecyl column and a 254-nm UV detector. The column was eluted with either ethanol/water (4:1) or isopropyl alcohol/water (3:2). Comparison of peak retention times with those of an authentic sample of benzyl ether indicated that in each case between 1 and 3 equiv of benzyl ether was detected.

Os(η^2-Fo-CHBA)$_2$-*trans*-(py)$_2$ (9′).[5] **Method a.** Os(η^4-CHBA-Et)(py)$_2$ (5) was oxidized by the same method used in the synthesis of **9** except that the CH_2Cl_2 contained 1 M *tert*-butyl alcohol or 1 M *tert*-amyl alcohol or was saturated with water; TLC indicated that the product was formed in high yield, but difficulty in purification and isolation produced a low yield (<30%) of the dark blue product: ^1H NMR (Table I). Anal. Calcd for $C_{26}H_{16}Cl_4N_4O_6Os$: C, 38.44; H, 1.99; N, 6.90. Found: C, 38.63; H, 2.16; N, 6.79.

Method b. Os(η^4-CHBA-Et)(py)$_2$ (5) (8 mg, 0.01 mmol) was dissolved in 10 mL of CH_2Cl_2 containing 0.5 M methanol and 2 M trifluoroacetic acid. To this solution was added a 0.1 M CH_2Cl_2 solution of tetrabutylammonium periodate which had been prepared from tetrabutylammonium hydroxide and periodic acid. TLC again indicated that **9′** was produced in high yield.

Os(η^4-CHBA-Et)(*t*-Bupy)$_2$ (5). K_2[Os(η^4-CHBA-Et)(O)$_2$]·$(H_2O)_4$ (3) (0.540 g) was dissolved in 15 mL of 4-*tert*-butylpyridine and 20 mL of H_2O. Triphenylphosphine (0.445 g, 2.5 equiv) was added to this inhomogeneous solution, and the resultant reaction mixture was treated as described for the unsubstituted pyridine adduct of **5**. This procedure yielded 0.505 g (84% based on **3**) of product as a dark blue microcrystalline solid. An analytical sample was obtained by purification on a preparatory TLC plate using CH_2Cl_2/THF (3:2) followed by recrystallization from CH_2Cl_2/pentane: ^1H NMR (Table I). Anal. Calcd for $C_{34}H_{34}Cl_4N_4O_4Os$: C, 45.54; H, 3.83; N, 6.26. Found: C, 45.56; H, 3.83; N, 6.23.

Os(η^4-CHBA-ethylene)(*t*-Bupy)$_2$ (7). Os(η^4-CHBA-Et)(*t*-Bupy)$_2$ (5) (100 mg) was heated on silica gel as described for the unsubstituted pyridine adduct of **7**. The product was removed from the silica as a bright yellow band by elution with CH_2Cl_2/acetone (9:1). Three fractions were collected as before and recrystallization from CH_2Cl_2 yielded the product as a very dark brown microcrystalline solid: yield 61 mg (61%). Anal. Calcd for $C_{34}H_{32}Cl_4N_4O_4Os$: C, 45.75; H, 3.61; N, 6.28. Found: C, 45.53; H, 3.63; N, 6.18.

Os(η^2-Fo-CHBA)-*cis*-(*t*-Bupy)$_2$ (9). Os(η^4-CHBA-Et)(*t*-Bupy)$_2$ (5) (50 mg, 0.050 mmol) was oxidized in the presence of methanol or isopropyl alcohol in the same manner used for the pyridine adduct of **9**. The product, which was isolated as before, contained significant amounts of the trans isomer, **9′**. The two compounds were separated on a preparative TLC plate (2000 µm, silica gel) by elution with CH_2Cl_2/THF (30:1). 32 mg (62%) of **9** was isolated as a dark blue powder from CH_2Cl_2/hexane. An analytical sample was obtained by slow crystallization from CH_2Cl_2/hexane: ^1H and ^{13}C NMR (Tables I and II). Anal. Calcd for $C_{34}H_{32}Cl_4N_4O_6Os$: C, 44.15; H, 3.49; N, 6.06. Found: C, 44.07; H, 3.68; N, 5.76.

Os(η^2-Fo-CHBA)-*trans*-(*t*-Bupy)$_2$ (9′). **Method a.** Os(η^4-CHBA-Et)(*t*-Bupy)$_2$ (5) (25 mg) was oxidized in the presence of 0.5 M *tert*-butyl alcohol with use of the same procedure as for the pyridine adducts of **9** and **9′**. TLC showed that the reaction was clean and that the product was formed in high yield. The high solubility of the dark blue compound led to a much lower yield of isolated material after recrystallization from boiling cyclohexane: yield 15 mg (58%); ^1H NMR (Table I). Anal. Calcd for $C_{34}H_{32}Cl_4N_4O_6Os$: C, 44.15; H, 3.49; N, 6.06. Found: C, 44.02; H, 3.53; N, 5.93.

Method b. Compound **9′** was formed as a minor product in the above synthesis of **9**. Ten milligrams (19%) of **9′** were recovered from the TLC separation of the two isomers.

K_2[Os(η^4-CHBA-DCB)(O)$_2$] (10). K_2[Os(OH)$_4$(O)$_2$] (1.345 g, 3.65 mmol) was dissolved in 150 mL of warm methanol, and the solution was then bubbled with N_2 for 30 min. H_4CHBA-DCB (2.00 g, 3.60 mmol) was dissolved in 100 mL of THF and also bubbled with N_2 for 0.5 h. The blue osmate solution was added to the ligand solution at room temperature immediately producing the deep orange color indicative of product formation. The solution was stirred for 10 min under N_2 and then evaporated to dryness. The product was dissolved in a minimum of THF, filtered, and dried over molecular sieves. Addition of hexane followed by removal of THF yielded the product as a brown microcrystalline solid. NMR indicated the presence of 1.5 molecules of H_2O per molecule of complex: yield 2.620 g (86%); ^1H NMR (Table I); IR (Nujol) 820 cm^{-1} (v s, $\nu_{as}(OsO_2)$). Anal. Calcd for $C_{20}H_6Cl_6K_2N_2O_6Os·1.5(H_2O)$: C, 27.40; H, 1.01; N, 3.20. Found: C, 27.60; H, 1.03; N, 3.19. Incorporation of ^{18}O was effected by dissolving the complex in dry THF, adding excess $H_2{}^{18}O$, and placing the solution under N_2 for 3 days: IR (Nujol)

782 cm^{-1} (v s, ν_{as}(Os^{18}O$_2$)).

Os(η^4-CHBA-DCB)(PPh$_3$)$_2$ (11). To a 50-mL Erlenmeyer flask with a stir bar were added K$_2$[Os(η^4-CHBA-DCB)(O)$_2$] (**10**) (221 mg, 0.260 mmol), triphenylphosphine (450 mg), ca. 5 mL of trifluoroacetic acid, and 10 mL of THF. The orange solution was heated until most of the THF had evaporated and a dark green molten triphenylphosphine mixture remained (ca. 10 min). After cooling, the mixture was dissolved in 10 mL of CH_2Cl_2 and the solution was placed on a short silica gel column. Elution with CH_2Cl_2 removed the product as a green band. Addition of hexane followed by removal of CH_2Cl_2 yielded the product as a dark green crystalline solid: yield 236 mg (72%); ^{1}H NMR (Table I). Anal. Calcd for $C_{56}H_{36}Cl_6N_2O_4OsP_2$: C, 53.14; H, 2.87; N, 2.21. Found: C, 53.33; H, 2.94; N, 2.22.

Os(η^4-CHBA-DCB)(*t*-Bupy)(PPh$_3$) (12). Os(η^4-CHBA-DCB)(PPh$_3$)$_2$ (**11**) (75 mg, 0.0593 mmol) was dissolved in 50 mL of CH_2Cl_2. Addition of 4-*tert*-butylpyridine followed by heating under reflux for 0.5 h produced a color change from dark green to light blue. Removal of solvents followed by recrystallization from CH_2Cl_2/hexane yielded the product as a dark blue crystalline solid. NMR showed the presence of 0.5 molecule of hexane per molecule of complex: yield 58 mg (86%); ^{1}H NMR (Table I). Anal. Calcd for $C_{47}H_{34}Cl_6N_3O_4OsP\cdot0.5(C_6H_{14})$: C, 50.82; H, 3.50; N, 3.56. Found: C, 50.72; H, 3.51; N, 3.53.

Os(η^4-CHBA-DCB)(*t*-Bupy)$_2$ (13). Os(η^4-CHBA-DCB)(PPh$_3$)$_2$ (**11**) (200 mg, 0.158 mmol) was dissolved in 20 mL of neat *t*-Bupy. The solution was heated under reflux for 15 min during which time the color changed from dark green to very dark blue, almost black. The *t*-Bupy was removed under vacuum and the crude product recrystallized from CH_2Cl_2/hexane. This yielded the pure product as a very dark crystalline solid. NMR showed the presence of 0.25 molecule of hexane per molecule of complex: yield 108 mg (68%); ^{1}H NMR (Table I). Anal. Calcd for $C_{38}H_{32}Cl_6N_4O_4Os\cdot0.25\ (C_6H_{14})$: C, 45.92; H, 3.46; N, 5.42. Found: C, 46.20; H, 3.52; N, 5.37.

Os(η^4-CHBA-DCB)(*t*-BuNC)$_2$ (14). K$_2$[Os(η^4-CHBA-DCB)(O$_2$)] (**10**) (120 mg, 0.135 mmol), triphenylphosphine (90 mg, 2.5 equiv), and *tert*-butyl isocyanide (0.20 mL, 12 equiv) were dissolved in 10 mL of THF and heated under reflux for 1.25 h. The solution was evaporated to dryness and the orange residue dissolved in CH_2Cl_2 and transferred to the top of a short silica gel column. The phosphine was removed by eluting with 300 mL of CH_2Cl_2, and the bright orange Os(III) intermediate was then removed with THF/acetone (1:1). This solution was concentrated and then treated with a dilute Br$_2$/THF solution at room temperature. The oxidation to the blue Os(IV) product was followed by TLC, and upon completion the reaction mixture was evaporated to dryness. The crude product was dissolved in 5 mL of CH_2Cl_2 and passed down a short silica gel column with CH_2Cl_2. Addition of hexane followed by removal of CH_2Cl_2 yielded the product as a dark blue crystalline solid: yield 20 mg (16%); ^{1}H NMR (Table I). Anal. Calcd for $C_{30}H_{24}Cl_6N_4O_4Os$: C, 39.71; H, 2.67; N, 6.17. Found: C, 39.75; H, 2.70; N, 6.19.

Os(η^4-CHBA-DCB)(bpy) (15). Os(η^4-CHBA-DCB)(PPh$_3$)$_2$ (**11**) (120 mg, 0.095 mmol) and bipyridine (210 mg, 1.34 mmol) were dissolved in toluene (10 mL) and heated under reflux for 0.5 h during which time the color darkened. The cooled solution was placed on a short silica gel column and eluted with excess CH_2Cl_2 to separate the product from starting material and 62 mg (78%) of product was isolated and recrystallized from CH_2Cl_2/hexane. Crystals for X-ray analysis were grown by vapor diffusion employing CH_2Cl_2/EtOH.

Acknowledgment. We acknowledge the donors of the Petroleum Research Fund, administered by the American Chemical Society, the Research Corporation, the Atlantic Richfield Corporation of America, and Occidental Research Inc. for support to T.J.C. and the National Science Foundation (Grant CHE-8107535 to T.J.C. and CHE 78-08716 to F.C.A.). S.L.G. is an NSF Predoctoral Fellow and T.E.K. is the Caltech Union Carbide Fellow in Chemical Catalysis. We thank John McNally for assistance with ligand preparations, Drs. William P. Schaefer and Richard E. Marsh for helpful discussions, and Engelhard Corporation for a generous donation of precious metal compounds. Operation of the Bruker WM-500 NMR spectrometer at the Southern California Regional NMR facility was supported by National Science Foundation Grant CHE-7916324.

Registry No. 1, 90791-62-1; **2**, 90791-63-2; **3**, 90791-45-0; **4**, 90791-46-1; **5** (L = py), 90791-47-2; **5** (L = *t*-Bupy), 90791-53-0; **7** (L = py), 90791-48-3; **7** (L = *t*-Bupy), 90791-54-1; **8a**, 90791-49-4; **8b**, 90791-50-7; **8***, 90791-51-8; **9** (L = py), 90865-92-2; **9** (L = *t*-Bupy), 90791-55-2; **9′** (L = py), 90791-52-9; **9′** (L = *t*-Bupy), 90865-47-7; **10**, 90791-56-3; **11**, 90791-57-4; **12**, 90791-58-5; **13**, 90791-59-6; **14**, 90791-60-9; **15**, 90791-61-0; TFA, 76-05-1; TBAP, 1923-70-2; H_4CHBA-ethylene, 90791-64-3; H_4CHBA-*t*-1,2-diMeO-Et, 90791-65-4; H_4CHBA-*t*-1,2-diEtO-Et, 90791-66-5; K$_2$[Os(OH)$_4$(O)$_2$], 77347-87-6; $^{18}O_2$, 32767-18-3; 2-acetylsalicyclic acid, 50-78-2; ethylenediamine, 107-15-3; 3,5-dichloroacetylsalicylic acid, 54223-75-5; 4,5-dichloro-*o*-phenylenediamine, 5348-42-5; tetrabutylammonium periodate, 65201-77-6.

Supplementary Material Available: Tables of data collection information, atom coordinates, Gaussian amplitudes, bond lengths and angles, and a listing of structure factor amplitudes (144 pages). Ordering information is given on any current masthead page.

Electrochemistry and Spectroelectrochemistry of σ-Bonded Iron Aryl Porphyrins. 1. Evidence for Reversible Aryl Migration from Iron to Nitrogen of Five-Coordinate Complexes

D. Lançon,[1a] **P. Cocolios,**[1a] **R. Guilard,**[1b] **and K. M. Kadish***[1a]

Contribution from the Department of Chemistry, University of Houston, Houston, Texas 77004, and the Laboratoire de Synthèse et d'Electrosynthèse Organométallique Associé au CNRS (LA 33), Faculté des Sciences "Gabriel", 21100 Dijon, France. *Received January 4, 1984*

Abstract: The iron aryl σ-bonded porphyrins (OEP)Fe(C_6H_5) and (TPP)Fe(C_6H_5) were studied by electrochemical and spectroelectrochemical techniques. Under appropriate conditions both complexes undergo one reversible single-electron reduction and two reversible single-electron oxidations. However, at slow scan rates the first oxidation process is followed by an irreversible chemical reaction producing a new electroactive species. This species may be further oxidized by one electron to yield the corresponding iron(III) *N*-phenyl derivative. The latter species is reversibly reduced by one electron to give $[(N\text{-}C_6H_5P)Fe^{II}]^+$, where P = OEP or TPP. This complex undergoes an overall two-electron irreversible reduction involving back-migration of the phenyl group from the nitrogen to the iron atom, thus generating the starting material in its reduced form.

During the past decade, studies of substrate activation by cytochrome P-450 have revealed the formation of σ-iron(III) alkyl (or aryl) P-450 complexes. Both in vivo experiments and use of model compounds have been carried out in order to elucidate the

0002-7863/84/1506-4472$01.50/0